Insight into Archean crustal growth and mantle evolution from multi-isotope U-Pb and Lu-Hf analysis of detrital zircon grains from the Abitibi and Pontiac subprovinces, Canada

Ben M Frieman, Nigel M Kelly, Yvette D Kuiper, Thomas Monecke, Andrew Kylander- Clark, Martin Guitreau

Highlights

- ~1,800 Lu-Hf/U-Pb analyses of detrital zircon from Archean successor basins
- Zircon isotopic signatures characterize Archean crust-mantle reservoirs
- Regional correlations reveal source domains in the Abitibi and adjacent subprovinces
- Data are consistent with existence of MORB-like depleted mantle by ~2950 Ma
- Results suggest presence of plate tectonic processes since the late-Mesoarchean

Insight into Archean crustal growth and mantle evolution from multi-isotope U-Pb and Lu-Hf analysis of detrital zircon grains from the Abitibi and Pontiac subprovinces, Canada

Ben M. Frieman[a,*], Nigel M. Kelly[a,b], Yvette D. Kuiper[a], Thomas Monecke[a], Andrew Kylander-Clark[c], Martin Guitreau[d]

[a] *Center for Mineral Resources Science, Department of Geology and Geological Engineering, Colorado School of Mines, Golden, CO 80401, United States*

[b] *Bruker Nano Analytics, 415 N Quay Street, Kennewick, WA 99336, United States*

[c] *Department of Earth Sciences, University of California, Santa Barbara, CA 93106, United States*

[d] *Laboratoire Magmas et Volcans, Université Clermont Auvergne, 63178 Aubière, France*

* Corresponding author.

E-mail address: bfrieman@laurentian.ca (B. Frieman).

Abstract

Lu-Hf laser ablation – multi-collector – inductively coupled plasma – mass spectrometry (LA-MC-ICP-MS) analysis was conducted on ~1,800 detrital zircon grains from successor basins of the Archean Abitibi and Pontiac subprovinces of Ontario and Quebec, Canada, and paired with previous U-Pb LA-MC-ICP-MS analyses of the same grains. Results are used to constrain the isotopic character of magmatic source domains of the zircon grains to establish the sedimentary provenance of the ~2690–2670 Ma successor basins, to provide constraints on terrane configurations and amalgamations at the time of basin formation, and to assess their significance for the record of crust-mantle growth in the region. The majority of results (95%) yield ε_{Hf} values of +1 to +10 for ~2850–2675 Ma zircon, and clusters along compositions of the Archean depleted mantle (DM), which is based on projections of modern MORB compositions. Subordinate results, comprising ~2% of the data set, yielded values (ε_{Hf} >+10) corresponding to extremely depleted mantle compositions, reflecting anomalously depleted sources in the ~2950–2670 Ma age range. The remaining 3% correspond to chondritic uniform reservoir (CHUR)-like to negative ε_{Hf} values that reflect primitive sources and/or evolved magmas in zircon that crystallized in the ~3250–3050 Ma and ~2950–2670 Ma age ranges. While Neoarchean grains dominate the data set (~88%), approximately 12% are Mesoarchean. The Lu-Hf data collected on these zircon grains, when compared with published isotopic results, preserve signatures indicative of derivation from exotic crustal domains juxtaposed during ~2690–2670 Ma amalgamation of the southern Superior Province. Since depleted compositions are characteristic of Neoarchean and Mesoarchean zircon groups in the southern Superior Province, and sources include local and distal domains that were likely separated by many 100s of kilometers prior to amalgamation, it is inferred that a depleted upper mantle reservoir was not only well-established, but prevalent in the mantle below each of these areas during their construction. Based on the predominant Hf isotope signatures in the detrital zircon results and predicted isotopic trends produced by probable geodynamic

mechanisms, crustal growth by direct differentiation from a depleted mantle reservoir is likely to have been moderated by subduction-accretion processes.

Keywords

Abitibi greenstone belt; Archean depleted mantle; Archean geodynamics; Crustal evolution

1. Introduction

Constraining the secular evolution of chemical composition and dynamics of the mantle is critical for the reconstruction of crustal growth processes through time (Korenaga, 2008; Fisher and Vervoort, 2018). The growth of continental crust in more recent geological times is generally accepted to have been driven by plate tectonic processes where much of the new continental crust is produced at convergent plate boundaries (Condie et al., 2011; Paterson et al., 2011). In a subduction setting, melts are predominantly extracted from a mantle with a time-integrated depletion history that reflects prior extraction of crust from the mantle at mid-ocean ridges (Hofmann, 1988; Griffin et al., 2002; Dhuime et al., 2011). However, it is unclear how applicable modern processes and their implied geodynamic settings are to the timing and processes of craton growth in early-Earth history (Smithies et al., 2005; Condie and Benn, 2006; Mueller and Wooden, 2012; Van Kranendonk et al., 2013; Bédard and Harris, 2014). The earliest evidence for Hadean to Eoarchean crust from the zircon record suggests derivation from a primitive, chondritic uniform reservoir (CHUR; Amelin et al., 1999; Kemp et al., 2010; Guitreau et al., 2012; Hiess and Bennett, 2016; Vezinet et al., 2018). In addition, the predominance of CHUR compositions in early-Earth zircon has been used, in part, to support the interpretation that Hadean to early Archean crustal growth occurred by derivation from a primitive mantle in plume-dominated regimes with little to no influence of older enriched crust or a coeval depleted mantle reservoir (Bédard, 2018; Fisher and Vervoort, 2018; Petersson et al., 2020). Where local signatures indicative of crustal differentiation from a depleted mantle (DM) reservoir are observed, the possible occurrence of nascent subduction has been invoked (Hoffmann et al., 2010). By the Neoarchean, evidence in crustal rocks for growth by derivation from a DM reservoir is more common (Guitreau et al., 2012). However, it is uncertain when the transition from CHUR to a globally extensive depleted upper mantle occurred. Placing constraints on the nature of, and processes associated with, the formation of the depleted mantle in the Meso- to Neoarchean is

67 therefore critical to understand this transition, which may relate to the onset of subduction-
68 accretion tectonic processes.

69 Hafnium isotopic studies on zircon are one of the most useful approaches to investigate
70 the chemical differentiation of crust and mantle. Such studies have provided insight into secular
71 interactions among crust-mantle reservoirs (Guitreau et al., 2012), supercontinent cycles and the
72 preservation potential of continental crust (Condie et al., 2011; Gardiner et al., 2016), and Hadean
73 crustal growth processes (Kemp et al., 2010). Zircon is uniquely suited for these studies as it
74 incorporates high Hf (weight percent) and low Lu (ppm) concentrations, thereby preserving an
75 initial Hf isotope ratio close to that of the parent magma. The timing of crystallization from the
76 parent magma can be independently constrained using the U-Pb isotopic system. The refractory
77 nature of zircon leads to preservation through weathering and erosion, and subsequent
78 concentration in clastic sedimentary rocks. This provides the potential to study the magmatic
79 evolution of a broader cross-section of contributing source terranes, some of which may no longer
80 be preserved at the surface. Consequently, the detrital zircon record has become an integral tool
81 for investigating the Hf isotope evolution of the crust and mantle (Iizuka et al., 2005; Condie et al.,
82 2011).

83 In this study, ~1,800 Lu-Hf analyses of zircon by laser ablation – multi-collector –
84 inductively coupled plasma – mass spectrometry (LA-MC-ICP-MS) are combined with existing U-
85 Pb LA-MC-ICP-MS data (Frieman et al., 2017) of detrital zircon grains from sedimentary rocks
86 deposited during the terminal stages of crustal amalgamation of the southern Superior Province
87 at ~2690–2670 Ma (Ayer et al., 2002; Davis, 2002; Percival et al., 2012). The detrital zircon record
88 of these sedimentary deposits constrains the crustal growth histories of the hinterland sources
89 where uplift and denudation were driven by terrane amalgamations (Frieman et al., 2017). Results
90 indicate that an isotopically distinct DM reservoir was regionally extensive beneath the different

components of the southern Superior Province throughout protracted construction of juvenile arc terranes during the Meso- to Neoarchean.

2. Regional geological framework

The Superior Province contains an extensive record of crustal growth spanning the Eo- to Neoarchean. A series of subprovinces and domains are identified that have distinct pre-amalgamation histories (Fig. 1; Stott et al., 2010). Furthermore, where common structural, magmatic, and isotopic histories are documented some of these have been grouped as composite regions (e.g., Percival et al., 2012).

2.1 Eo- to Mesoarchean rocks of the Superior Province

The oldest rocks of the Superior Province are Eo- to Paleoarchean (>3800–3200 Ma) and occur in the Hudson Bay region and Minnesota River Valley subprovince (Figs. 1 and 2). The Quebec portion of the Hudson Bay region contains ~3800–3400 Ma gneissic-plutonic rocks (Cates et al., 2013; O'Neil et al., 2013; Böhm et al., 2019) that display Nd and Hf isotopic signatures indicative of derivation from primitive mantle sources. Neodymium isotope anomalies suggest localized mixing with ~4300–3800 Ma source rocks (O'Neil et al., 2013; Guitreau et al., 2013; O'Neil and Carlson, 2017; Böhm et al., 2019), indicating the potential for a preserved Hadean history. At the northwestern extent of the Hudson Bay region in Ontario, gneissic (paragneiss and orthogneiss) and tonalite-trondhjemite-granodiorite (TTG) intrusive rocks of the Assean Lake Complex occur (Fig. 1). The paragneiss units contain xenocrystic zircon cores with ~3850–3200 Ma U-Pb ages and the ~3200 Ma orthogneiss and TTG units display whole-rock Nd model ages of >4000 Ma, which do not clearly correlate to known Eo- to Paleoarchean domains in the Superior Province (Böhm et al., 2019; Vezinet et al., 2020). Gneissic-plutonic rocks of the

115 Minnesota River Valley subprovince have ~3500–3100 Ma U-Pb magmatic zircon crystallization
116 ages (Fig. 2; Bickford et al., 2006) in rocks with mantle extraction ages of ~3750–3500 Ma
117 (Satkoski et al., 2013).

118 While Eoarchean rocks are not spatially extensive, many domains contain a record of
119 Paleo- to Mesoarchean (~3600–2800 Ma) crustal genesis (Figs. 1 and 2). These include the
120 Arnaud River and North Caribou regions, the Winnipeg River and Marmion subprovinces of the
121 southwestern Superior region, the Hawk domain within the Wawa subprovince, and the Opatica
122 subprovince of the Moyen-Nord region (Fig. 1). The Arnaud River region contains inherited zircon
123 and Nd model ages of ~2920–2800 Ma (Fig. 2; Percival et al., 2012). The North Caribou region
124 forms the core of the northwestern Superior Province composed of Mesoarchean crustal
125 components (Davis et al., 2005), which are characterized by 3000–2800 Ma volcanic-plutonic
126 rocks with juvenile Nd signatures (Percival et al., 2012). The Winnipeg River subprovince is cored
127 by ~3325–2825 Ma tonalitic rocks that yield evolved Nd and Hf isotopic signatures with model
128 ages up to ~3500 Ma (Fig. 2; Henry et al., 2000; Davis et al., 2005; Bjorkman, 2017), potentially
129 representing a rifted component of the North Caribou region (Davis et al., 2005). The Marmion
130 subprovince contains ~3000–2800 Ma volcanic-plutonic rocks with juvenile, depleted mantle Hf
131 and Nd signatures (Tomlinson et al., 2004; Davis et al., 2005; Melnyk et al., 2006; Bjorkman,
132 2017). Rare Mesoarchean rocks occur as ~2820 Ma tonalitic rocks of the Opatica subprovince
133 (Davis et al., 1994) as well as in ~2900–2800 Ma gneissic-plutonic rocks of the Hawk domain
134 where an isolated fragment of older crust is exposed within the Wawa subprovince (Figs. 1 and
135 2; Turek et al., 1992; Moser et al., 1996; Ketchum et al., 2008).

136

137 2.2 Neoarchean rocks of the Superior Province

Neoarchean volcanic-plutonic successions in the Superior Province unconformably overlie and/or are structurally interleaved with Eo- to Mesoarchean rocks (Percival et al., 2012). However, many domains contain no older components and represent Neoarchean juvenile crust. These domains now comprise large proportions of the central to southern Superior Province, including the majority of the Moyen-Nord region, and the western Wabigoon, Wawa, and Abitibi subprovinces (Fig. 1). In these domains, extensive magmatism resulted in the formation of juvenile greenstone belts and the intrusion of coeval TTG complexes. Formation of greenstone belts occurred at ~2795–2755 Ma in the Opatica subprovince (Davis et al., 1994), ~2775–2720 Ma in the western Wabigoon subprovince (Davis et al., 2005), ~2720–2700 Ma in the Eastmain subprovince (Goutier et al., 1999), ~2720 Ma in the Wawa subprovince (Corfu and Stott, 1998) and ~2795–2695 Ma in the Abitibi subprovince (Mortensen, 1993; Ayer et al., 2002; Thurston et al., 2008; Leclerc et al., 2012). Whole-rock and single mineral isotopic (Hf and Nd) and geochemical analyses indicate that greenstone belts were primarily derived from juvenile, depleted mantle sources that may represent intraoceanic arc to back-arc complexes (Smith et al., 1987; Henry et al., 2000; Ayer et al., 2002; Polat and Kerrich, 2002; Davis et al., 2005; Lodge, 2016; Bjorkman, 2017).

2.3 Successor basins in the Superior Province

Sedimentary successor basins are common throughout the Superior Province. These include regional (100s of km) to local (10s of km) sedimentary deposits that formed at <2750–2670 Ma (Fig. 2; Percival et al., 2012). Successor basin formation postdates igneous construction of local volcanic supracrustal units by millions of years and is temporally associated with deformation driven by amalgamation. The timing of deposition in individual successor basins has been constrained by their youngest detrital zircon populations and/or by the age of cross-cutting igneous rocks (Fig. 2), with current estimates of ~2720–2710 Ma in the English River and North Caribou region (Davis et al., 2005), ~2715–2700 Ma in the southwestern Superior region

(including the western Wabigoon, Winnipeg River, and Marmion subprovinces; Stott et al., 2002; Sanborn-Barrie and Skulski, 2006), ~2715–2695 Ma in the Moyen-Nord region (Cleven et al., 2020), ~2700–2690 Ma in the Quetico and northern Abitibi subprovinces (Davis et al., 1990; David et al., 2007), and ~2690–2670 Ma in the Wawa, southern Abitibi, and Pontiac subprovinces (Mortensen and Card, 1993; Corfu and Stott, 1998; Ayer et al., 2002; Davis, 2002). Successor basin deposits are progressively younger from north to south, reflecting propagation of the regional deformation front during Neoarchean amalgamation (Davis, 2002; Percival et al., 2012; Frieman et al., 2017).

2.4 Geology of the Abitibi and Pontiac subprovinces

The Abitibi subprovince in the southern Superior Province (Fig. 1) is one of the largest and best-preserved greenstone belts in the world (Monecke et al., 2017). Supracrustal rocks include ~2795–2695 Ma submarine mafic to felsic volcanic successions (Figs. 2 and 3; Mortensen, 1993; Ayer et al., 2002; Thurston et al., 2008; Leclerc et al., 2012; McNicoll et al., 2014; Mathieu et al., 2020) consisting of basalt-komatiite and basalt-rhyolite associations that may have formed in arc-related settings (Dostal and Mueller, 1997; Ayer et al., 2002; Polat and Kerrich, 2006).

Plutonic rocks occur as syn-volcanic, syn-deformational, and post-deformational intrusions (Ayer et al., 2002; Monecke et al., 2017). Syn-volcanic intrusions display compositions similar to coeval volcanic units and occur as spatially restricted ~2795–2695 Ma complexes (Corfu, 1993; Mortensen, 1993; Ayer et al., 2002; Monecke et al., 2017). Syn-deformational intrusions are ~2690–2670 Ma and include TTG, monzonite, syenite, granite, and diorite (Corfu, 1993; Mortensen, 1993; Ayer et al., 2002; McNicoll et al., 2014). Post-deformational intrusions are ~2670–2650 Ma and are dominated by granite (Monecke et al., 2017).

Whole-rock and single mineral Nd and Hf isotopic studies indicate that magma sources to the volcanic-plutonic rocks display juvenile (depleted) signatures and record no significant interaction with older crustal material (Cattell et al., 1984; Shirey and Hanson, 1986; Corfu and Noble, 1992; Vervoort et al., 1994; Ayer et al., 2002). This has led to the interpretation that they formed in an oceanic basin setting prior to accretion with the Superior Province (Ayer et al., 2002; Polat and Kerrich, 2006). However, rare ~2900–2800 Ma inherited xenocrystic zircon grains have been documented (Ayer et al., 2002; Ketchum et al., 2008), possibly indicating that the Abitibi subprovince formed proximal to a Mesoarchean crustal fragment, perhaps represented by the Hawk domain (Ketchum et al., 2008) and/or the Opatica subprovince (Davis et al., 1994).

Two distinct successor basin successions are recognized in the southern Abitibi subprovince (Fig. 3), which formed in response to progressive deformation driven by collision of the Abitibi subprovince with domains to the north at ~2690–2670 Ma (Ayer et al., 2002; Davis, 2002). The Porcupine assemblage, a subaqueous, turbidite-dominated sedimentary succession, was deposited at ~2690–2685 Ma (Ayer et al., 2002; Davis, 2002) during the initial phases of deformation, while the Timiskaming assemblage, a subaqueous to subaerial, coarse clastic-dominated sedimentary succession, was deposited during later stages of deformation at ~2679–2669 Ma (Corfu, 1993; Ayer et al., 2002; Davis, 2002). The Porcupine assemblage disconformably overlies the ~2750–2695 Ma volcanic assemblages whereas the Timiskaming assemblage unconformably overlies all older rocks of the Abitibi subprovince (Monecke et al., 2017).

Sedimentary rocks of the Pontiac subprovince located immediately to the south of the Abitibi subprovince (Figs. 1 and 3) consist of ~2685–2682 Ma, predominately turbidite successions (Mortensen and Card 1993; Davis, 2002), displaying similar sedimentological characteristics to the Porcupine assemblage. They were intruded by post-deformational (2660–2640 Ma) granitic batholiths (Fig. 3; Mortensen and Card, 1993; Davis, 2002).

Samples from successor basins of the Abitibi and Pontiac subprovinces display broadly similar detrital zircon age patterns (Davis, 2002; Frieman et al., 2017), defined by a majority (80–95%) of Neoarchean and subordinate amount (5–20%) of Mesoarchean grains (Frieman et al., 2017). Similarities are interpreted to reflect the persistence of relatively local and shared provenance domains throughout their deposition at ~2690–2670 Ma. However, the younger Timiskaming assemblage deposits contain a higher proportion of Mesoarchean zircon grains relative to the older Porcupine and Pontiac successor basins, which likely reflects greater inputs from distal sources as regional amalgamation and hinterland emergence progressed (Frieman et al., 2017).

3. Methods

Zircon grains from sixteen samples, originally collected for U-Pb dating (Frieman et al., 2017) were analyzed for Lu-Hf isotopes - six samples from the Porcupine assemblage, eight from the Timiskaming assemblage and two from the Pontiac subprovince (Table 1, Fig. 3). Sample descriptions and details on the sampling methodology and zircon separation techniques are given in Frieman et al. (2017). All samples yielded heavy mineral separates from which >125 zircon grains were mounted in epoxy plugs and polished to half depth. Back-scattered electron (BSE), secondary electron (SE), and panchromatic cathodoluminescence (CL) images were collected for each mount at the U.S. Geological Survey in Lakewood, Colorado, using a JOEL 5800LV scanning electron microscope (SEM) operated at 15 kV and 5 nA. Additional BSE and SE imaging was conducted at the Department of Geology and Geological Engineering, Colorado School of Mines, using a TESCAN MIRA3 field emission-scanning electron microscope operated at 15 kV and 11 nA. The SEM images were used to select the location of analytical spots. Where possible, analytical spots were placed in zones representing magmatic growth such as simple oscillatory or sector zoning (Fig. 4).

Isotopic analyses were conducted by LA-MC-ICP-MS at the University of California Santa Barbara, using a Nu Plasma multi-collector coupled to a Photon Machines Excite 193 nm laser-ablation system, following the procedures of Kylander-Clark et al. (2013). The U-Pb and Lu-Hf isotopes were measured during separate analytical sessions. Initially, the U-Pb laser spots (~15 µm) were placed and then the Lu-Hf spots (~40–50 µm) were overlain or placed directly adjacent within the same textural domain (Fig. 4).

The U-Pb analyses used here are a subset of those reported by Frieman et al. (2017) on which Lu-Hf analyses were performed. The U-Pb data were processed in Iolite *v2.5* (Paton et al., 2011) where the time-integrated signals for each ablation period were assessed for isotopic and trace element homogeneity. Where compositional heterogeneity was observed, either the spot analysis was rejected or the signal was clipped to only include the homogenous portion of the isotopic signals. For additional details concerning the collection and post-processing of the U-Pb data the reader is referred to Frieman et al. (2017). Where U-Pb analyses were more than >5% discordant, the U-Pb and corresponding Lu-Hf data were rejected from further analysis. The accepted data are provided in Supplemental Table 1. Uncertainties are reported as 2σ, unless stated otherwise.

The Hf isotope data were normalized using an exponential mass bias correction and a natural $^{179}Hf/^{177}Hf$ ratio of 0.7325 (Stevenson and Patchett, 1990). Isobaric interferences of ^{176}Yb and ^{176}Lu on ^{176}Hf were corrected using $^{173}Yb/^{171}Yb$ and $^{176}Yb/^{173}Yb$ values of 1.123575 and 0.786847 (Thirlwall and Anczkiewicz, 2004), respectively, as well as a $^{176}Lu/^{175}Lu$ value of 0.02655 (Vervoort et al., 2004). Secondary reference materials used included 91500, GJ-1, Plešovice, Mud Tank, Mun-3, and Mun-4 (Wiedenbeck et al., 1995; Morel et al., 2008; Sláma et al., 2008; Fisher et al., 2011). Each reference material yielded weighted-mean $^{176}Hf/^{177}Hf$ ratios within 1-3% of the accepted value indicating that isobaric interferences were well-corrected. The mass-corrected $^{176}Lu/^{177}Hf$ isotopic ratios were used to calculate the initial $^{176}Hf/^{177}Hf$ ratios and ε_{Hf}

values at the time of crystallization, based on the U-Pb age (Supplemental Table 1). The reported uncertainty on the initial $^{176}Hf/^{177}Hf$ ratios and ε_{Hf} values includes propagation of the 2σ uncertainty on the measured $^{176}Lu/^{177}Hf$ ratios and the $^{207}Pb/^{206}Pb$ dates calculated in quadrature. The ^{176}Lu decay constant of $1.867 \pm 8 \times 10^{-11}$ (Söderlund et al., 2004) and CHUR values of $^{176}Lu/^{177}Hf$ = 0.0338 and $^{176}Hf/^{177}Hf$ = 0.282793 were used (Iizuka et al., 2015). The resultant initial $^{176}Hf/^{177}Hf$ ratios and ε_{Hf} values are plotted against the isotope evolution curves for the DM and CHUR. The depleted mantle curve was calculated based on the modern MORB-DM values of ε_{Hf} = +17, $^{176}Lu/^{177}Hf$ = 0.0384, and $^{176}Hf/^{177}Hf$ = 0.283250 (Griffin et al., 2002), using the aforementioned ^{176}Lu decay constant. To visualize the high density of data, the ε_{Hf} – $^{207}Pb/^{206}Pb$ age results are also presented as a bivariate histogram plot, which was constructed using standard Matlab routines with 10 Ma and 0.5 ε_{Hf} unit bin spacing. The statistical distribution of the results was assessed using HafniumPlotter v1.7 (Sundell et al., 2019). In this application, each data point is converted to a 3D Gaussian and plotted on a 512 by 512 cell grid using the aforementioned kernel density bandwidth to produce a bivariate data density map. This data density map was then contoured to display the ≥95% and ≥68% data density intervals of the results.

4. U-Pb and Lu-Hf isotopic results

The U-Pb ages discussed here are from only those zircon grains analyzed by Frieman et al. (2017) for which paired Lu-Hf spot analyses were also obtained. These results consist of 1790 U-Pb determinations that met the filtering criterion given above. Detrital zircon data from the Abitibi and Pontiac subprovince samples are grouped together since they are interpreted to have a shared provenance (Frieman et al., 2017) and, thus, can collectively be used to constrain crustal growth processes that occurred in the inferred source domains. A frequency histogram, a normalized probability density curve, and a cumulative probability density curve for these data are

displayed in Figure 5A. The U-Pb age data are ~12% Mesoarchean and ~88% Neoarchean, displaying a prominent peak at ~2715 Ma (Fig. 5A).

The initial $^{176}Hf/^{177}Hf$ ratios for all analyses are between 0.280667 and 0.281464 with an average uncertainty of ± 0.000093 (Supplemental Table 1). They correspond to ε_{Hf} values between -6.5 to +17.2 with a mean of +5.3, although the majority of the data (n=1641) fall between +2 and +10 ε_{Hf} units (Fig. 6). The 2σ uncertainty on the ε_{Hf} data, including covariance on all parameters, ranges from 1.5 to 9.3 ε_{Hf} units with a mean uncertainty of 3.3 epsilon units.

To facilitate discussion, analyses are subdivided into six groups (Fig. 6). Group 1 comprises the largest proportion of results (n=1693; 95%) and is defined by the dominant statistical population from the Gaussian, bivariate kernel density distribution of the results (Fig. 6B). This group forms a large cluster of data that plots between 2850 Ma and 2670 Ma with ε_{Hf} values of +0.5 to +9.5. Group 1a comprises a subgroup that contains 68% (n=1211) of the results, defining a peak cluster that plots between 2750 Ma and 2690 Ma with ε_{Hf} values of +2.5 to +8. The remaining 5% of the results were split into five distinct groups based on similar U-Pb age and ε_{Hf} distributions (i.e., groups 2–6; Fig. 6B). Group 2 is defined by zircon grains with ε_{Hf} values similar to group 1 (ε_{Hf} of +2 to +8), but lie outside the 95% confidence interval and spread to older ages up to ~3000 Ma. Group 3 is defined by data that display lower ε_{Hf} values that plot below the 3100 Ma crustal evolution line and display ages of ~2950–2670 Ma. These have been subdivided into two groups. Group 3a represents a younger cluster that yields ages of ~2800–2670 Ma (n=16). Group 3b (n=18) represents an older population in the 2950–2800 Ma age range. Group 4 (n=6) is defined by analyses that plot below the DM curve (ε_{Hf} values of +4 to -1) and display U-Pb ages of ~3250–3000 Ma. Groups 5 and 6 are defined by clusters of data that largely yield ε_{Hf} values of > +9 (Fig. 6), with group 5 (n=30) composed of ~2950–2670 Ma zircon grains and group 6 (n=9) of ~3150–2950 Ma zircon grains.

5. Discussion

5.1 Lu-Hf data trends and regional correlations

Newly acquired Lu-Hf isotopic analyses are coupled with previously published U-Pb isotopic analyses of detrital zircon grains from successor basins of the Abitibi and Pontiac subprovinces. This data set represents the largest and most comprehensive multi-isotope detrital zircon data set compiled to date for rocks within the southern Superior Province. It provides constraints on the isotopic character of source rocks to successor basin sedimentary deposits.

The U-Pb age patterns of successor basin detrital zircon grains from the Abitibi and Pontiac subprovinces indicate that these rocks were derived from a mixture of both local and distal sources (Fig. 5B; Davis, 2002; Frieman et al., 2017). In part, this interpretation is based on the presence of Mesoarchean zircon grains in the successor basin sedimentary rocks and the absence of volcanic-plutonic rocks of this age in the Abitibi and Pontiac subprovinces (Fig. 5). Zircon grains with U-Pb ages that are ≥2800 Ma account for ~12% of the total data set (n=215; Fig. 5A), requiring a substantial component of mixing between local, <2800 Ma and distal, >2800 Ma sources to produce the observed age spectra (Fig. 5B). Statistical comparisons with published zircon age data from the southern Superior Province suggest that the occurrence of ‘exotic’ Mesoarchean zircon grains are best explained by sources from areas juxtaposed during amalgamation at ~2690–2670 Ma, such as the Winnipeg River, Marmion, and Opatica subprovinces (Fig. 5B; Frieman et al., 2017). The absence of any Eo- to Paleoarchean components in the Abitibi successor basin sedimentary rocks implies that sources from terranes of the northern Superior Province were unlikely (Frieman et al., 2017) or contributed negligible components. The new Lu-Hf data paired with previously published U-Pb data provide a means to assess the validity of this interpretation.

Of the Lu-Hf results obtained in this study, group 1 (~2850–2670 Ma) represents the majority of data (95%) and is likely to reflect a mixture of local Abitibi, and distal non-Abitibi subprovince sources (Fig. 5; Frieman et al., 2017). These results cluster near DM-like compositions with a subordinate spread towards more distributed ε_{Hf} values between +10 and +0.5 (Fig. 6). Group 1a zircon grains are 2750–2680 Ma and have ε_{Hf} values between +8 and +2.5 (Fig. 6). Volcanic-plutonic rocks of the Abitibi subprovince are ~2795–2695 Ma in age (Fig. 5B) with the oldest, ~2795–2760 Ma units being restricted to the northern Abitibi subprovince (Vervoort et al., 1994; David et al., 2007; Mathieu et al., 2020). Previously published zircon data for Abitibi subprovince igneous rocks yielded ε_{Hf} values of -4 to +11, with the majority of results clustering between +2 and +7 (Figs. 7A and 8; Corfu and Noble, 1992; Ketchum et al., 2008), consistent with the ε_{Hf}-age distributions observed in group 1a (Figs. 6B and 8). The whole-rock Nd data primarily display ε_{Nd} values of 0 to +5 (Fig. 7C), similar to the dominant population observed in the zircon Hf data (Figs. 6 and 7A; Cattell et al., 1984; Dupré et al., 1984; Shirey and Hanson, 1986; Walker et al., 1988; Vervoort et al., 1994; Vervoort and Blichert-Toft, 1999). Thus, the dominant proportion of the results (group 1a; Fig. 6) are interpreted to reflect local derivation from the Neoarchean igneous source rocks that make up the Abitibi subprovince, similar to previous interpretations (Davis, 2002; Frieman et al., 2017). However, Neoarchean igneous rocks with comparable depleted Hf and Nd isotopic compositions are also abundant in the Wawa (Smith et al., 1987; Henry et al., 2000; Polat and Kerrich, 2002), western Wabigoon (Henry et al., 2000; Davis et al., 2005; Bjorkman, 2017), and Marmion (Tomlinson et al., 2004; Davis et al., 2005; Bjorkman, 2017) subprovinces (Figs. 7 and 8). Consequently, some of the detrital zircon grains in group 1a may have also been derived from adjacent domains (the Wawa subprovince) or those juxtaposed during regional amalgamation (the western Wabigoon, Winnipeg River, and Marmion subprovinces), as has been previously interpreted from the U-Pb age patterns (Frieman et al., 2017).

Since no rocks older than ~2800 Ma occur in the Abitibi subprovince (Fig. 5B; Monecke et al., 2017) the ~3000–2800 Ma zircon grains (Fig. 6) were likely sourced from juxtaposed domains that also contain a history of Mesoarchean crustal genesis. We suggest that the Marmion subprovince is the most probable source for these grains, because volcanic-plutonic rocks of the Marmion subprovince contain evidence for partial derivation from a DM reservoir at ~3000–2800 Ma (Figs. 7B, 7D, and 8; Tomlinson et al., 2004, Davis et al., 2005; Melnyk et al., 2006; Bjorkman, 2017), providing a potential source that is consistent with the results observed in group 2 (Fig. 6). Alternatively, the Hawk domain (Figs. 1 and 2) may have constituted a proximal source of detritus. The extent of this domain is poorly constrained, but is interpreted to extend from the western portion of the Abitibi subprovince (Ketchum et al., 2008) through the Paleoproterozoic Kapuskasing uplift (Moser et al., 1996) to present-day exposures of ~3000–2900 Ma gneissic-plutonic rocks in the eastern part of the Wawa subprovince (Turek et al., 1992). Inherited zircon grains that have ages of ~2925 Ma and ~2860–2850 Ma have been reported from ~2740–2700 Ma volcanic-plutonic rocks of the Abitibi subprovince (Ayer et al., 2002; Ketchum et al., 2008) and may have been derived from the Hawk domain or equivalent lower crustal components in the southern Superior Province. However, it is unlikely that zircon grains derived from the Hawk domain significantly contributed to our samples, since these rocks may have been exhumed relatively late in the amalgamation history at ~2615 Ma (Turek et al., 1992) and, thus, were not extensively exposed at the time of successor basin formation (Frieman et al., 2017).

The more evolved (low positive to negative) ε_{Hf} values of groups 3 and 4 (Fig. 6) may reflect interactions with Mesoarchean and older crust in source domains of the successor basin sedimentary rocks as they plot along the 3500–3100 Ma ε_{Hf} evolution lines for Superior Province crust ($^{176}Lu/^{177}Hf$ = 0.015; Stevenson and Patchett, 1990). This suggests that zircon grains of groups 3 and 4 may have crystallized from magmas either derived directly from melting of older sources or from primitive mantle melts that partially mixed with these magmas (Fig. 8). These

associations suggest that rocks from which these zircon grains were derived may contain a late Paleo- to Mesoarchean crustal component and/or reflect a component of older (>3000 Ma) CHUR-derived mantle melts (Fig. 8). A potential source for detrital zircon grains with this signature is from the Winnipeg River subprovince, which contains an older (~3500–3000 Ma), evolved basement component (Fig. 7B and D; Davis et al., 2005; Bjorkman, 2017). Therefore, it is inferred that groups 3 and 4 (Fig. 6) represent sources from the southwest Superior Province such as the Winnipeg River and Marmion subprovinces (Fig. 8).

Detrital zircon grains with ε_{Hf} values of ≤0 and U-Pb ages of ~3200–2900 Ma and ~2700 Ma have been observed in sedimentary rocks of the intervening Quetico subprovince (Fig. 7B; Davis et al., 2005) and may have constituted a source for zircon grains in groups 3 and 4 of the samples investigated in this study (Fig. 6). The Marmion and Winnipeg River subprovinces likely were the primary sources for detritus in the Quetico subprovince during deposition at ~2700–2690 Ma (Fralick et al., 2006). However, due to its impingement between the Wawa and Marmion/western Wabigoon subprovinces, sedimentation in the Quetico subprovince ceased at ~2690 Ma as it began to experience deformation, uplift, and erosion (Corfu and Stott, 1998; Sanborn-Barrie and Skulski, 2006). Thus, starting at ~2690 Ma, following initiation of deposition in the successor basins of the Abitibi and Pontiac subprovinces, detrital zircon grains with Meso- to Neoarchean ages and evolved isotopic signatures were more likely derived directly from erosion of the Winnipeg River and Marmion subprovinces, or indirectly from other exotic domains to the north (e.g., the North Caribou region; Fig. 1) through recycling of the Quetico subprovince sedimentary rocks (Frieman et al., 2017).

While statistically minor (<2%), the > +10 ε_{Hf} values documented for group 5 (Fig. 6) are enigmatic as anomalously depleted signatures are rare in Meso- to Neoarchean rocks worldwide (Guitreau et al., 2012). However, elevated ε_{Hf} signatures represent a subordinate proportion of Hf isotope results from the Yilgarn craton of western Australia (Mole et al., 2019) and have been

observed in the Superior Province. For example, ε_{Hf} values as high as +8 to +12 have been reported from whole-rock and zircon samples from the Abitibi and Wawa subprovinces (Figs. 7A and 8; Smith et al., 1987; Ketchum et al., 2008). It has been proposed that these ε_{Hf} values reflect derivation from melt sources in the upper mantle to lower crust that experienced prior melt histories and therefore have highly depleted compositions (Smith et al., 1987). In this interpretation, melts sourced from garnet-rich residues, which have elevated Lu-Hf ratios due to preferential partitioning of Lu into garnet, may inherit anomalously high ε_{Hf} (Zheng et al., 2005; Hoffmann et al., 2010). Therefore, we interpret the ε_{Hf} values > +10 to reflect derivation from volumetrically minor crustal or mantle regions that were locally supra-depleted as a result of multi-stage melt histories (Fig. 8).

While groups 1–5 can be interpreted within the framework of the published isotopic data and geological history of the southern Superior Province (Fig. 7), data from group 6 are not consistent with the published data as they display anomalously depleted (> +10 ε_{Hf}) isotopic signatures in the ~3150–2950 Ma age range (Fig. 6). It is possible that they may correlate with undocumented lithologies, reflect multi-stage melt processes, and/or represent artifacts of data reduction. An assessment of U-Th-Pb data following the method of Guitreau and Flahaut (2019) was carried out to compare measured $^{232}Th/^{238}U$ ratios with time-integrated $^{232}Th/^{238}U$ ratios calculated using $^{208}Pb/^{206}Pb$ ratios and $^{207}Pb/^{206}Pb$ ages (Fig. 9). While rare in other groups (Fig. 9A-B), analyses in group 6 display calculated $^{232}Th/^{238}U$ ratios that are high relative to measured ratios, suggesting that these results are likely affected by common Pb contamination (Fig. 9C) and the measured U-Pb ages for these grains are likely overestimated.

5.2 Significance of Lu-Hf results to the record of crust-mantle reservoirs in the southern Superior Province

Our data set is dominated by late Meso- to Neoarchean zircon grains with ε_{Hf} signatures that are moderately to strongly depleted (ε_{Hf} of +4 to +8), displaying values that plot near a predicted MORB-DM projection (Fig. 6). As discussed above and based on evaluation of the U-Pb ages (Frieman et al., 2017), a significant proportion of these zircon grains were likely derived from proximal sources within the Abitibi subprovince. Abundant geochronology in the Abitibi subprovince indicates that it is composed solely of Neoarchean (~2795–2670 Ma) rocks (Fig. 5B; Monecke et al., 2017), and previously reported Hf and Nd isotopic results indicate a primarily juvenile, isotopically depleted source for these rocks (Fig. 7A and C; Cattell et al., 1984; Dupré et al., 1984; Shirey and Hanson, 1986; Walker et al., 1988; Corfu and Noble, 1992; Vervoort et al., 1994; Vervoort and Blichert-Toft, 1999). However, minimal contamination from older, 2900–2800 Ma crust has been inferred based on lower observed ε_{Hf} values (Ketchum et al., 2008). Thus, the existing evidence is consistent with the interpretation that igneous rocks of the Abitibi subprovince were primarily derived from a moderately to strongly depleted mantle reservoir with typical ε_{Hf} values of +4 to +8.

The presence of Mesoarchean ages in the detrital zircon populations documented here (Fig. 5A) cannot be explained by local provenance. Instead, this requires derivation from exotic domains of the southern Superior Province that were juxtaposed with the Abitibi subprovince during regional amalgamation (Figs. 5B and 8; Frieman et al., 2017; see section 5.1). Potential source domains include the western Wabigoon, Winnipeg River, and Marmion subprovinces. These domains each contain abundant Neoarchean rocks that yield zircon Hf and whole-rock Nd isotopic compositions indicative of crustal generation from a DM reservoir (ε_{Hf} of +3 to +6 and ε_{Nd} values of +2 to +4; Figs. 7B, 7D, and 8; Tomlinson et al., 2004; Davis et al., 2005; Bjorkman, 2017). Therefore, they are also interpreted to have contributed zircon to group 1a (Figs. 6 and 8). The consistently depleted character of isotopic signatures from Neoarchean volcanic-plutonic rocks has been noted by previous authors (Corfu and Noble, 1992; Davis et al., 2005) and is well-

represented in the statistically dominant populations in the data from this (Fig. 6) and previous studies, regardless of location within the southern Superior Province (Fig. 8). Thus, it is possible that juvenile crust formed in disparate domains throughout the southern Superior Province was largely derived from similar, geochemically distinct DM reservoirs that may have been local or regional in extent.

In Proterozoic and younger settings, it is well established that the evolution of crust and mantle reservoirs is predominately moderated by plate tectonic processes where geochemically differentiated crust and depleted mantle are complementary (Hofmann, 1988). While the operation of plate tectonic processes in the Archean is uncertain (Smithies et al., 2005; Piper, 2013; Bédard and Harris, 2014; Bédard, 2018; Petersson et al., 2020), it has been proposed that subduction may have been transient (Moyen and van Hunen, 2012), producing isolated mantle domains with DM-like signatures. Alternatively, Archean geodynamic processes may have included more sustained plate tectonics with long-lived subduction (Shirey et al., 2008) that produced a regional to globally extensive depleted mantle reservoir. In the absence of a plate tectonic model, it has been proposed that whole mantle-scale overturn/upwelling events (Stein and Hofmann, 1994; Bédard and Harris, 2014; Bédard, 2018) with intervening periods of stagnant-lid behavior (Piper, 2013; Bédard, 2018), or the upwelling of smaller-scale plumes similar to modern ocean island basalt settings (Mueller and Wooden, 2012; Van Kranendonk et al., 2013; Petersson et al., 2020), were largely responsible for crustal growth and the resultant geochemical record in crust and mantle reservoirs.

Based on differing processes of crust-mantle growth, predictions can be made about the resultant geochemical signatures, providing a framework to evaluate the operation of the various geodynamic models. Early in Earth's history, owing to periods of inefficient to restricted mantle convection and the presence of stagnant crustal lids, the mantle may have developed periodic instabilities and undergone whole mantle-scale overturn/upwelling events (Piper, 2013; Bédard

and Harris, 2014). The recurrence of these events has been invoked to explain the global record of episodic crustal growth in the Hadean to early Archean (Griffin et al., 2014; Bédard, 2018) and has been proposed as a mechanism to explain widespread Neoarchean (~2800–2700 Ma) crustal genesis in the Superior Province (Bédard and Harris, 2014). In this model, magmas are formed above the upwelling zone through high degrees of decompression melting. Furthermore, pre-existing crustal domains above the upwelling zone would be strongly reworked, undergoing magmatic underplating, crustal delamination, and/or intra-continental rifting. Therefore, isotopic signatures of any new crust formed in these domains would either record the primitive signature of the upwelling mantle or display evolved, negative ε_{Hf} signatures of the reworked crustal material. This type of Hf isotope signature is well-documented in magmatic rocks of the Paleoproterozoic Bushveld large igneous province that has been interpreted to have formed during a ~2060 Ma superplume event (Rajesh et al., 2013; Zirakparvar et al., 2019). These rocks display ε_{Hf} values that range from -3 to -21 and are interpreted to reflect the mixing of deeply sourced primitive mantle inputs with pre-existing continental crust and/or sublithospheric mantle (Zirakparvar et al., 2019), consistent with the framework described above. Consequently, the long-term effect of a superplume or mantle overturn event would be to produce crust and mantle domains that display a predominately primitive (CHUR-like) signature or more evolved (strongly negative) ε_{Hf} signatures due to reworking of this material. This is due to the fact that upwelling will transport large volumes of primitive lower mantle material to the upper mantle, either homogenizing the upper mantle to a CHUR-like lower mantle, or strongly shifting the bulk upper mantle towards this primitive composition. As a result, ongoing crustal growth would display a shift toward predominately primitive Hf compositions.

The detrital zircon isotope results indicate that juvenile, ~3000–2700 Ma crust primarily records ε_{Hf} values of +4 to +8 (Fig. 6) and similarly depleted signatures are observed throughout the southern Superior Province (e.g., Fig. 8; Corfu and Noble, 1992; Ayer et al., 2002; Tomlinson

et al., 2004; Davis et al., 2005; Bjorkman, 2017), indicating that crustal differentiation occurred by derivation from a DM reservoir. If late Meso- to Neoarchean crust of the southern Superior Province was primarily derived from a mantle overturn/upwelling system, a larger proportion of zircon with CHUR-like or negative ε_{Hf} values would be expected. However, this is not observed (Fig. 8). It is also possible that smaller-scale mantle plumes similar to modern ocean island basalt settings contributed to crustal growth processes in the Archean (Smithies et al., 2005; Mueller and Wooden, 2012; Van Kranendonk et al., 2013). However, similar to the overturn/upwelling model, primary melts derived from a plume source are predicted to display a CHUR-like primitive mantle signature, and melts influenced by any secondary mixing or magma differentiation processes would display an evolved (negative) isotopic signature. This type of ε_{Hf} signature is observed in a statistically less significant proportion of the detrital zircon data set (group 3; Figs. 6 and 8). Thus, if present, plume-derived melts were minor in volume compared with magmas derived from the depleted mantle. This suggests that the negative ε_{Hf} signatures are a result of secondary processes such as mixing of juvenile magmas with those derived from older crust and/or crustal reworking/amalgamations (Fig. 8). The detrital zircon data suggest that protracted to episodic growth from a well-established, regional DM reservoir occurred over time-frames spanning 100s of millions of years in the late Mesoarchean to Neoarchean (Fig. 8). Therefore, it is difficult to reconcile the observed data from the southern Superior Province with sustained to intermittent periods of mantle overturn or plume activity that would have resulted in crustal differentiation from a predominately primitive mantle reservoir with a CHUR-like composition. As a result, it is likely that an alternative geodynamic mechanism played a significant role in late Archean crustal growth in the southern Superior Province, which is further discussed below.

It is possible that modern-style plate tectonic processes were in operation during Archean crustal construction and amalgamation of the southern Superior Province (Dostal and Mueller, 1997; Ayer et al., 2002; Polat and Kerrich, 2002, 2006; Benn and Moyen, 2008; Polat, 2009;

Percival et al., 2012; Lodge, 2016; Frieman et al., 2017). In Proterozoic and younger settings, juvenile arc terranes commonly display depleted isotopic signatures with temporal shifts towards more evolved (CHUR-like to negative) ε_{Hf} values due to magmatism during later internal reworking, perhaps driven by collisional events (Guitreau et al., 2014; Gardiner et al., 2016). In this model, the predominately depleted Hf signatures of detrital zircon in this study (group 1; Fig. 6) represent magmatism in juvenile arc to back-arc complexes that formed by partial melting at subduction zones from a regional or, perhaps, globally extensive DM reservoir. While it is possible that long-lived subduction was responsible for the development and geochemical maintenance of the observed depleted upper mantle reservoir (Shirey et al., 2008), it is also possible that intermittent subduction (Silver and Behn, 2008) contributed to its formation and secular evolution. Furthermore, in the subduction model, the subordinate non-DM-like populations, including those that display less-depleted to negative values (groups 3 and 4; Fig. 6) are interpreted to reflect magmatic reworking and/or Neoarchean or earlier arc accretion processes (Fig. 8). Regardless, the less-depleted to negative isotopic data represent a small proportion of the overall results (<3%; Fig. 8; Supplemental Table 1), indicating that reworking and/or mixing with older crustal reservoirs within the juvenile terranes was minimal, possibly due to the short-lived nature of the arcs and/or their strongly depleted character. This type of signature dominates the juvenile, Neoarchean domains of the southern Superior Province such as the Abitibi, Wawa, and western Wabigoon subprovinces, where amalgamations of arc to back-arc complexes is inferred to have occurred shortly after their initial formation (Dostal and Mueller, 1997; Ayer et al., 2002; Polat and Kerrich, 2002, 2006; Benn and Moyen, 2008; Polat, 2009; Percival et al., 2012; Lodge, 2016; Frieman et al., 2017). In addition to contributions from older crustal material, these amalgamation events have been invoked to explain evolved compositions observed in their Hf isotope record (Davis et al., 2005; Ketchum et al., 2008; Bjorkman, 2017). It is possible that the CHUR-like to negative results observed in >3000 Ma zircon (Fig. 8) reflect non-plate tectonic processes and that these processes may have contributed to the formation of the observed late Mesoarchean to

559 Neoarchean DM reservoir. However, the paucity of Hf data from early to middle Mesoarchean
560 detrital and igneous zircon makes inferences about the earlier evolution of the crust and mantle
561 associated with the southern Superior Province difficult.

562 The data presented here record no evidence for a temporal progression from CHUR
563 towards DM compositions in the upper mantle during late Meso- to Neoarchean volcano-plutonic
564 construction in the southern Superior Province, and no coeval complementary enriched reservoir
565 in the crustal record is observed (Figs. 6 and 7). Thus, it is unlikely that the depleted signature
566 was locally restricted. While depleted Hf isotope signatures dominate Neoarchean signatures
567 (Figs. 6, 7, and 8), the trends become less clear in the Mesoarchean. The detrital zircon data
568 contain a large population of grains with depleted Hf isotope signatures in the ~3000–2800 Ma
569 age range (group 2; Fig. 6). Corresponding isotopic signatures in zircon of this age range are
570 defined by more limited clusters of previously reported zircon Hf and whole-rock Nd data (Figs. 7
571 and 8). For example, for the southwestern Superior Province, data cluster along ε_{Hf} values of +3
572 to +5 in the 3000–2800 Ma age range (Fig. 8). In part, these results correspond to those of slivers
573 of supracrustal rocks in the Marmion subprovince that comprise the Lumby Lake greenstone belt
574 (Tomlinson et al., 2004; Bjorkman, 2017). While these contain an earlier, Mesoarchean (3000–
575 2800 Ma) record of juvenile crustal growth from a DM-like reservoir (Henry et al., 2000; Tomlinson
576 et al., 2004; Davis et al., 2005), they also contain more evolved isotopic signatures due to the
577 mixing and amalgamation with older, Paleoarchean crust of the Winnipeg River subprovince (Fig.
578 8; Davis et al., 2005; Bjorkman, 2017). Due to earlier amalgamation events and/or localized
579 mixing with older crust, this depleted mantle signature is less well defined in the previously
580 published data (Fig. 7) than it is in the late Mesoarchean (~2950–2800 Ma) detrital zircon data
581 (Fig. 6), perhaps, suggesting that a preservation bias exists in present-day exposures.
582 Regardless, the combined igneous and detrital zircon record support the presence of a DM

583 reservoir throughout late Meso- to Neoarchean crustal growth in the southern Superior Province
584 (Fig. 8).

585 The magnitudes of separation between the southern Superior Province source domains
586 prior to their amalgamation in the Neoarchean are unknown (Percival et al., 2012). However,
587 based on their present-day configuration, an estimate of the amount of shortening recorded
588 (~50%) across the terranes, and a >25 Myr record of convergence defined by amalgamation
589 events from ~2715 Ma in the Winnipeg River and western Wabigoon subprovinces to ~2690 Ma
590 in the Abitibi and Wawa subprovinces (Percival et al., 2012), the terranes were potentially several
591 thousands of kilometers apart (assuming conservative convergence rates of 60 km/Myr) prior to
592 their amalgamation. Based on this interpretation and the broad area of provenance observed, we
593 suggest that a DM-like reservoir was not only well-established within the mantle beneath each of
594 the domains within the southern Superior Province when they formed, but was pervasive in the
595 mantle by the late Meso- to Neoarchean and, as a result, may reflect a predominance of modern-
596 style plate tectonic processes at this time.

597

598 **6. Conclusions**

599 The ~1,800 paired U-Pb and Lu-Hf analyses of detrital zircon grains from successor basins
600 of the Abitibi and Pontiac subprovinces represent the most comprehensive single multi-isotope
601 detrital zircon data set in the region. The dominant portion of the data yield moderately to strongly
602 depleted Hf isotope compositions that are interpreted to reflect repeated crustal growth from a
603 well-established, DM reservoir. The subordinate CHUR-like or more evolved results are best
604 explained by a combination of reworking after short-lived (<50 Ma) crustal residence and local
605 derivation from or mixing with magmas derived from older, Mesoarchean crust. Anomalously
606 depleted data are interpreted in terms of volumetrically minor crustal or mantle sources that

retained multi-stage melt histories. Through a comparison to the regional geology and the previously published isotopic record, potential local and distal detrital zircon sources are identified throughout the southern Superior Province. These include the western Wabigoon, Winnipeg River, Marmion, Quetico, and Wawa subprovinces. Based on these regional correlations, we suggest that the protracted record of late Mesoarchean to Neoarchean crustal growth recorded in the southern Superior Province occurred by differentiation from a well-established, isotopically distinct, and regionally extensive depleted mantle reservoir. Since a depleted signature is dominant and no temporal progression from CHUR-like values or a coeval complementary enriched reservoir is observed, it is suggested that non-plate tectonic processes alone cannot explain the observed trends. A model where subduction-accretion plate tectonic processes occurred during widespread late Meso- to Neoarchean crustal genesis is favored.

Acknowledgments

Samples collection at Hoyle Pond and Kidd Creek was logistically supported by E. Barr and T. Gemmell, respectively. We thank B. Wares for his helpful comments on the geology of the Abitibi subprovince and ongoing interest in the results of this research. The research was financially supported by Osisko Mining. Additional support included graduate student research grants from the Society of Economic Geologists Canada Foundation and the Geological Society of America awarded to B. Frieman and Colorado School of Mines professional development funds to Y. Kuiper. We thank Drs. A. Petersson, A. Vezinet, and N. Wodicka for their insightful comments that helped us improve the final version of this manuscript.

References

Amelin, Y., Lee, D.C., Halliday, A.N., Pidgeon, R.T., 1999. Nature of the Earth's earliest crust from hafnium isotopes in single detrital zircons. Nature 399, 252–255.

Ayer, J.A., Dostal, J., 2000. Nd and Pb isotopes from the Lake of the Woods greenstone belt, northwestern Ontario: Implications for mantle evolution and the formation of crust in the southern Superior Province. Can. J. Earth Sci. 37, 1677–1689. doi:10.1139/e00-067

Ayer, J., Amelin, Y., Corfu, F., Kamo, S., Ketchum, J., Kwok, K., Trowell, N., 2002. Evolution of the southern Abitibi greenstone belt based on U-Pb geochronology: Autochthonous volcanic construction followed by plutonism, regional deformation and sedimentation. Precambrian Res. 115, 63–95. doi:10.1016/S0301-9268(02)00006-2

Beakhouse, G.P., McNutt, R.H., 1991. Contrasting types of late Archean plutonic rocks in northwestern Ontario: Implications for crustal evolution in the Superior Province. Precambrian Res. 49, 141–165.

Bédard, J.H., 2018. Stagnant lids and mantle overturns: Implications for Archaean tectonics, magmagenesis, crustal growth, mantle evolution, and the start of plate tectonics. Geosci. Front. 9, 19–49.

Bédard, J.H., Harris, L.B., 2014. Neoarchean disaggregation and reassembly of the Superior craton. Geology 42, 951–954. doi:10.1130/G35770.1

Benn, K., Moyen, J.F., 2008. The late Archean Abitibi-Opatica terrane, Superior Province: A modified oceanic plateau. Geol. Soc. Amer. Spec. Pap. 440, 173–197.

Bickford, M.E., Wooden, J.L., Bauer, R.L., 2006. SHRIMP study of zircons from Early Archean rocks in the Minnesota River Valley: Implications for the tectonic history of the Superior Province. Geol. Soc. Amer. Bull. 118, 94–108.

651 Bjorkman, K.E, 2017. 4D crust-mantle evolution of the western Superior Craton: Implications for
652 Archaean granite-greenstone petrogenesis and geodynamics. University of Western
653 Australia, Unpublished PhD thesis, 313 p. doi:10.4225/23/5a39c88a2f559

654 Böhm, C.O., Hartlaub, R.P., Heaman, L.M., Cates, N., Guitreau, M., Bourdon, B., Roth, A.S.G.,
655 Mojzsis, S.J., Blichert-Toft, J., 2019. The Assean Lake Complex: Ancient crust at the
656 northwestern margin of the Superior Craton, Manitoba, Canada. In: Van Kranendonk, M.J.
657 et al. (Eds) Earth's Oldest Rocks (Second Edition). Elsevier, 703–722.

658 Bouvier, A., Vervoort, J.D., Patchett, P.J., 2008. The Lu-Hf and Sm-Nd isotopic composition of
659 CHUR: Constraints from unequilibrated chondrites and implications for the bulk
660 composition of terrestrial planets. Earth Planet. Sci. Lett. 273, 48–57.

661 Cattell, A., Krough, T.E., Arndt, N.T., 1984. Conflicting Sm-Nd whole rock and U-Pb ages for
662 Archean lavas from Newton Township, Abitibi belt, Ontario. Earth Planet Sci. Lett. 70,
663 280–290.

664 Cates, N.L., Ziegler, K., Schmitt, A.K., Mojzsis, S.J., 2013. Reduced, reused and recycled: Detrital
665 zircons define a maximum age for the Eoarchean (ca. 3750–3780 Ma) Nuvvuagittuq
666 supracrustal belt, Québec (Canada). Earth Planet. Sci. Lett. 362, 283–293.

667 Cleven, N.R., Guilmette, C., Davis, D.W., Côté-Roberge, M., 2020. Geodynamic significance of
668 Neoarchean metasedimentary belts in the Superior Province: Detrital zircon U-Pb LA-ICP-
669 MS geochronology of the Opinaca and La Grande subprovinces. Precambrian Res. 347,
670 105819. doi:10.1016/j.precamres.2020.105819

671 Condie, K.C., Benn, K., 2006. Archean geodynamics: Similar to or different from modern
672 geodynamics? Geophys. Monogr. Ser. 164, 47–59.

673 Condie, K.C., Bickford, M.E., Aster, R.C., Belousova, E., Scholl, D.W., 2011. Episodic zircon
674 ages, Hf isotopic compositions, and the preservation rate of continental crust. Geol. Soc.
675 Amer. Bull. 123, 951–957.

676 Corfu, F., 1993. The evolution of the southern Abitibi greenstone belt in light of precise U-Pb
677 geochronology. Econ. Geol. 88, 1323–1340.

678 Corfu, F., Noble, S.R., 1992. Genesis of the southern Abitibi greenstone belt, Superior Province,
679 Canada: Evidence from zircon Hf isotope analyses using a single filament technique.
680 Geochim. Cosmochim. Acta 56, 2081–2097.

681 Corfu, F., Stott, G.M., 1998. Shebandowan greenstone belt, western Superior Province: U-Pb
682 ages, tectonic implications, and correlations. Geol. Soc. Amer. Bull. 110, 1467–1484.
683 doi:10.1130/0016-7606(1998)110<1467:SGBWSP>2.3.CO;2

684 David, J., Davis, D.W., Dion, C., Goutier, J., Legault, M., Roy, P., 2007. Datations U-Pb effectuées
685 dans la Sous-province de l'Abitibi en 2005–2006. Ministère des Ressources naturelles et
686 de la Faune du Québec, RP 2007-01, 17 p.

687 Davis, D.W., 2002. U-Pb geochronology of Archean metasedimentary rocks in the Pontiac and
688 Abitibi subprovinces, Quebec, constraints on timing, provenance and regional tectonics.
689 Precambrian Res. 115, 97–117. doi:10.1016/S0301-9268(02)00007-4

690 Davis, D.W., Pezzutto, F., Ojakangas, R.W., 1990. The age and provenance of metasedimentary
691 rocks in the Quetico subprovince, Ontario, from single zircon analyses: Implications for
692 Archean sedimentation and tectonics in the Superior Province. Earth Planet. Sci. Lett. 99,
693 195–205. doi:10.1016/0012-821X(90)90110-J

694 Davis, W.J., Gariépy, C., Sawyer, E.W., 1994. Pre-2.8 Ga crust in the Opatica gneiss belt: A
695 potential source of detrital zircons in the Abitibi and Pontiac subprovinces, Superior
696 Province, Canada. Geology 22, 1111–1114.

697 Davis, D.W., Amelin, Y., Nowell, G.M., Parrish, R.R., 2005. Hf isotopes in zircon from the western
698 Superior province, Canada: Implications for Archean crustal development and evolution
699 of the depleted mantle reservoir. Precambrian Res. 140, 132–156.
700 doi:10.1016/j.precamres.2005.07.005

701 DePaolo, D.J., Wasserburg, G.J., 1976. Nd isotopic variations and petrogenetic models.
702 Geophys. Res. Lett. 3, 249–252.

703 Dhuime, B., Hawkesworth, C., Cawood, P., 2011. When continents formed. Science 331, 154–
704 155.

705 Dostal, J., Mueller, W.U., 1997. Komatiite flooding of a rifted Archean rhyolitic arc complex:
706 Geochemical signature and tectonic significance of the Stoughton-Roquemaure Group,
707 Abitibi greenstone belt, Canada. J. Geol. 105, 545–563.

708 Dupré, B., Chauvel, C., Arndt, N.T., 1984. Pb and Nd isotopic study of two Archean komatiites
709 flows from Alexo, Ontario. Geochim. Cosmochim. Acta 48, 1965–1972.

710 Fisher, C.M., Vervoort, J.D., 2018. Using the magmatic record to constrain the growth of
711 continental crust—the Eoarchean zircon Hf record of Greenland. Earth Planet. Sci. Lett.
712 488, 79–91.

713 Fisher, C.M., Hanchar, J.M., Samson, S.D., Dhuime, B., Blichert-Toft, J., Vervoort, J.D., Lam, R.,
714 2011. Synthetic zircon doped with hafnium and rare earth elements: A reference material
715 for in situ hafnium isotope analysis. Chem. Geol. 286, 32–47.

716 Fralick, P., Purdon, R.H., Davis, D.W., 2006. Neoarchean trans-subprovince sediment transports
717 in the southwestern Superior Province: Sedimentological, geochemical, and
718 geochronological evidence. Can. J. Earth Sci. 43, 1055–1070.

719 Frieman, B.M., Kuiper, Y.D., Kelly, N.M., Monecke, T., Kylander-Clark, A., 2017. Constraints on
720 the geodynamic evolution of the southern Superior Province: U-Pb LA-ICP-MS analysis
721 of detrital zircon in successor basins of the Archean Abitibi and Pontiac subprovinces of
722 Ontario and Quebec, Canada. Precambrian Res. 292, 398–416.

723 Gardiner, N.J., Kirkland, C.L., Van Kranendonk, M.J., 2016. The juvenile hafnium isotope signal
724 as a record of supercontinent cycles. Sci. Rep. 6, 38503. doi:10.1038/srep38503

725 Goutier, J., Dion, C., David, J., Dion, D.J., 1999. Géologie de la région de la passe Shimusuminu
726 et du lac Vion (33F/11 et 33F/12). Ministère des Ressources naturelles du Québec, RG
727 98-17, 41 p.

728 Griffin, W.L., Wang, X., Jackson, S.E., Pearson, N.J., O'Reilly, S.Y., Xu, X., Zhou, X., 2002. Zircon
729 chemistry and magma mixing, SE China: In-situ analysis of Hf isotopes, Tonglu and
730 Pingtan igneous complexes. Lithos 61, 237–269.

731 Griffin, W.L., Belousova, E.A., O'Neill, C., O'Reilly, S.Y., Malkovets, V., Pearson, N.J., Spetsius,
732 S., Wilde, S.A., 2014. The world turns over: Hadean Archean crust mantle evolution. Lithos
733 189, 2–15.

734 Guitreau, M., Flahaut, J., 2019. Record of low-temperature aqueous alteration of Martian zircon
735 during the late Amazonian. Nature Comm. 10, 2457. doi:10.1038/s41467-019-10382-y

736 Guitreau, M., Blichert-Toft, J., Martin, H., Mojzsis, S.J., Albarède, F., 2012. Hafnium isotope
737 evidence from Archean granitic rocks for deep-mantle origin of continental crust. Earth
738 Planet. Sci. Lett. 337–338, 211–223.

739 Guitreau, M., Blichert-Toft, J., Mojzsis, S.J., Roth, A.S.G., Bourdon, B., 2013. A legacy of Hadean
740 silicate differentiation inferred from Hf isotopes in Eoarchean rocks of the Nuvvuagittuq
741 supracrustal belt (Québec, Canada). Earth Planet. Sci. Lett. 362, 171–181.

742 Guitreau, M., Blichert-Toft, J., Billström, K., 2014. Hafnium isotope evidence for early-Proterozoic
743 volcanic arc reworking in the Skellefte district (northern Sweden) and implications for the
744 Svecofennian orogen. Precambrian Res. 252, 39–52.

745 Henry, P., Stevenson, R.K., Larbi, Y., Gariépy, C., 2000. Nd isotopic evidence for Early to Late
746 Archean (3.4–2.7 Ga) crustal growth in the western Superior Province (Ontario, Canada).
747 Tectonophysics 322, 135–151.

748 Hiess, J., Bennett, V.C., 2016. Chondritic Lu/Hf in the early crust–mantle system as recorded by
749 zircon populations from the oldest Eoarchean rocks of Yilgarn Craton, West Australia and
750 Enderby Land, Antarctica. Chem. Geol. 427, 125–143.

751 Hoffmann, J.E., Münker, C., Polat, A., König, S., Mezger, K., Rosing, M.T., 2010. Highly depleted
752 Hadean mantle reservoirs in the sources of early Archean arc-like rocks, Isua supracrustal
753 belt, southern West Greenland. Geochim. Cosmochim. Acta 74, 7236–7260.

754 Hofmann, A.W., 1988. Chemical differentiation of the Earth: The relationship between mantle,
755 continental crust, and oceanic crust. Earth Planet. Sci. Lett. 90, 297–314.

756 Iizuka, T., Hirata, T., Komiya, T., Rino, S., Katayama, I., Motoki, A., Maruyama, S., 2005. U-Pb
757 and Lu-Hf isotope systematics of zircons from the Mississippi river sand: Implications for
758 reworking and growth of continental crust. Geology 33, 485–488.

759 Iizuka, T., Yamaguchi, T., Hibiya, Y., Amelin, Y., 2015. Meteorite zircon constraints on the bulk
760 Lu-Hf isotope composition and early differentiation of the Earth. Proc. Natl. Acad. Sci.
761 U.S.A. 112, 5331–5336.

762 Kemp, A.I.S., Wilde, S.A., Hawkesworth, C.J., Coath, C.D., Nemchin, A., Pidgeon, R.T., Vervoort,
763 J.D., DuFrane, S.A., 2010. Hadean crustal evolution revisited: New constraints from Pb-
764 Hf isotope systematics of the Jack Hills zircons. Earth Planet. Sci. Lett. 296, 45–56.

765 Ketchum, J.W.F., Ayer, J.A., van Breemen, O., Pearson, N.J., Becker, J.K., 2008. Pericontinental
766 crustal growth of the southwestern Abitibi subprovince, Canada – U-Pb, Hf, and Nd
767 isotope evidence. Econ. Geol. 103, 1151–1184. doi:10.2113/gsecongeo.103.6.1151

768 Korenaga, J., 2008. Urey ratio and the structure and evolution of Earth's mantle. Rev. Geophys.
769 46, RG2007. doi:10.1029/2007RG000241

770 Kylander-Clark, A.R.C., Hacker, B.R., Cottle, J.M., 2013. Laser-ablation split-stream ICP
771 petrochronology. Chem. Geol. 345, 99–112. doi:10.1016/j.chemgeo.2013.02.019

772 Larbi, Y., Stevenson, R., Breaks, F., Machado, N., Gariépy, C., 1999. Age and isotopic
773 composition of late Archean leucogranites: Implications for continental collision in the
774 western Superior Province. Can. J. Earth Sci. 36, 495–510.

775 Leclerc, F., Harris, L.B., Bédard, J.H., van Breemen, O., Goulet, N., 2012. Structural and
776 stratigraphic controls on magmatic, volcanogenic, and shear zone-hosted mineralization
777 in the Chapais-Chibougamau mining camp, northeastern Abitibi, Canada. Econ. Geol.
778 107, 963–989.

779 Lodge, R.W.D., 2016. Petrogenesis of intermediate volcanic assemblages from the
780 Shebandowan greenstone belt, Superior Province: Evidence for subduction during the
781 Neoarchean. Precambrian Res. 272, 150–167. doi:10.1016/j.precamres.2015.10.018

782 Mathieu, L., Snyder, D.B., Bedeaux, P., Cheraghi, S., Lafrance, B., Thurston, P., Sherlock, R.,
783 2020. Deep into the Chibougamau area, Abitibi greenstone belt: Structure of a

784 Neoarchean crust revealed by seismic reflection profiling. Tectonics 39, e2020TC006223.
785 doi:10.1029/2020TC006223

786 McNicoll, V., Goutier, J., Dubé, B., Mercier-Langevin, P., Ross, P.S., Dion, C., Monecke, T.,
787 Legault, M., Percival, J., Gibson, H., 2014. U-Pb geochronology of the Blake River Group,
788 Abitibi greenstone belt, Quebec, and implications for base metal exploration. Econ. Geol.
789 109, 27–59.

790 Melnyk, M., Davis, D.W., Cruden, A.R., Stern, R.A., 2006. U-Pb ages constraining structural
791 development of an Archean terrane boundary in the Lake of the Woods area, western
792 Superior Province, Canada. Can. J. Earth Sci. 43, 967–993. doi:10.1139/E06-035

793 Mole, D.R., Kirkland, C.L., Fiorentini, M.L., Barnes, S.J., Cassidy, K.F., Isaac, C., Belousova, E.A.,
794 Hartnady, M., Thebaud, N., 2019. Time-space evolution of an Archean craton: A Hf-
795 isotope window into continent formation. Earth-Sci. Rev. 196, 1–46, 102831.
796 doi:10.1016/j.earscirev.2019.04.003

797 Monecke, T., Mercier-Langevin, P., Dubé, B., Frieman, B.M., 2017. Geology of the Abitibi
798 greenstone belt. Rev. Econ. Geol. 19, 7–49.

799 Morel, M.L.A., Nebel, O., Nebel-Jacobsen, Y.J., Miller, J.S., Vroon, P.Z., 2008. Hafnium isotope
800 characterization of the GJ-1 zircon reference material by solution and laser-ablation MC-
801 ICPMS. Chem. Geol. 255, 231–235. doi:10.1016/j.chemgeo.2008.06.040

802 Mortensen, J.K., 1993. U-Pb geochronology of the eastern Abitibi subprovince. Part 1:
803 Chibougamau-Matagami-Joutel region. Can. J. Earth Sci. 30, 11–28.

804 Mortensen, J.K., Card, K.D., 1993. U-Pb age constraints for the magmatic and tectonic evolution
805 of the Pontiac subprovince, Quebec. Can. J. Earth Sci. 30, 1970–1980.

806 Moser, D.E., Heaman, L.M., Krogh, T.E., Hanes, J.A., 1996. Intracrustal extension of an Archean
807 orogen revealed using single-grain U-Pb zircon geochronology. Tectonics 15, 1093–1109.

808 Moyen, J.F., van Hunen, J., 2012. Short-term episodicity of Archaean plate tectonics. Geology
809 40, 451–454.

810 Mueller, P.A., Wooden, J.L., 2012. Trace element and Lu-Hf systematics in Hadean-Archean
811 detrital zircons: Implications for crustal evolution. J. Geo. 120, 15–29.

812 O'Neil, J., Carlson, R.W., 2017. Building Archean cratons from Hadean mafic crust. Science 355,
813 1199–1202.

814 O'Neil, J., Boyet, M., Carlson, R.W., Paquette, J.L., 2013. Half a billion years of reworking of
815 Hadean mafic crust to produce the Nuvvuagittuq Eoarchean felsic crust. Earth Planet. Sci.
816 Lett. 379, 13–25.

817 Paterson, S.R., Okaya, D., Memeti, V., Economos, R., Miller, R.B., 2011. Magma addition and
818 flux calculations of incrementally constructed magma chambers in continental margin
819 arcs: Combined field, geochronologic, and thermal modeling studies. Geosphere 7, 1439–
820 1468.

821 Paton, C., Hellstrom, J., Paul, B., Woodhead, J., Hergt, J., 2011. Iolite: Freeware for the
822 visualization and processing of mass spectrometric data. J. Anal. At. Spectrom. 26, 2508–
823 2518.

824 Pearson, D.G., Shirey, S.B., Carlson, R.W., Boyd, F.R., Pokhilenko, N.P, Shimizu, N., 1995. Re-
825 Os, Sm-Nd, and Rb-Sr isotope evidence for thick Archaen lithospheric mantle beneath the
826 Siberian craton modified by multistage metasomatism. Geochim. Cosmochim. Acta 59,
827 959–977.

828 Percival, J.A., Skulski, T., Sanborn-Barrie, M., Stott, G.M., Leclair, A.D., Corkery, M.T., Boily, M.,
829 2012. Geology and tectonic evolution of the Superior Province, Canada. Geol. Assoc.
830 Can. Spec. Pap. 49, 321–378.

831 Petersson, A., Kemp, A.I.S., Gray, C.M., Whitehouse, M.J., 2020. Formation of early Archean
832 granite-greenstone terranes from a globally chondritic mantle: Insights from igneous rocks
833 of the Pilbara Craton, Western Australia. Chem. Geol. 551, 119757.
834 doi:10.1016/j.chemgeo.2020.119757

835 Piper, J.D.A., 2013. A planetary perspective on Earth evolution: Lid tectonics before plate
836 tectonics. Tectonophysics 589, 44–56.

837 Polat, A., 2009. The geochemistry of Neoarchean (ca. 2700 Ma) tholeiitic basalts, transitional to
838 alkaline basalts, and gabbros, Wawa subprovince, Canada: Implications for petrogenetic
839 and geodynamic processes. Precambrian Res. 168, 83–105.

840 Polat, A., Kerrich, R., 2002. Nd-isotope systematics of ~2.7 Ga adakites, magnesian andesites,
841 and arc basalts, Superior Province: Evidence for shallow crustal recycling at Archean
842 subduction zones. Earth Planet. Sci. Lett. 202, 345–360.

843 Polat, A., Kerrich, R., 2006. Regarding the geochemical fingerprints of Archean hot subduction
844 volcanic rocks: Evidence for accretion and crustal recycling in a mobile tectonic regime.
845 Geophys. Monogr. Ser. 164, 189–213.

846 Rajesh, H.M., Chisonga, B.C., Shindo, K., Beukes, N.J., Armstrong, R.A., 2013. Petrographic,
847 geochemical and SHRIMP U-Pb titanite age characterization of the Thabazimbi mafic sills:
848 Extended time frame and a unifying petrogenetic model for the Bushveld large igneous
849 province. Precambrian Res. 230, 79–102.

850 Sanborn-Barrie, M., Skulski, T., 2006. Sedimentary and structural evidence for 2.7 Ga continental
851 arc-oceanic-arc collision in the Savant-Sturgeon greenstone belt, western Superior
852 Province, Canada. Can. J. Earth Sci. 43, 995–1030. doi:10.1139/E06-060

853 Satkoski, A.M., Bickford, M.E., Samson, S.D., Bauer, R.L., Mueller, P.A., Kamenov, G.D., 2013.
854 Geochemical and Hf-Nd isotopic constraints on the crustal evolution of Archean rocks from
855 the Minnesota River Valley, USA. Precambrian Res. 224, 36–50.

856 Shirey, S.B., Hanson, G.N., 1986. Mantle heterogeneity and crustal recycling in Archean granite-
857 greenstone belts: Evidence from Nd isotopes and trace elements in the Rainy Lake area,
858 Superior Province, Ontario, Canada. Geochim. Cosmochim. Acta 50, 2631–2651.

859 Shirey, S.B., Kamber, B.S., Whitehouse, M.J., Mueller, P.A., Basu, A.R., 2008. A review of the
860 isotopic and trace element evidence for mantle and crustal processes in the Hadean and
861 Archean: Implications for the onset of plate tectonic subduction. Geol. Soc. Amer. Spec.
862 Pap. 440, 1–29.

863 Silver, P.G., Behn, M.D., 2008. Intermittent plate tectonics? Science 319, 85–88.

864 Sláma, J., Košler, J., Condon, D.J., Crowley, J.L., Gerdes, A., Hanchar, J.M., Horstwood, M.S.A.,
865 Morris, G.A., Nasdala, L., Norberg, N., Schaltegger, U., Schoene, B., Tubrett, M.N.,
866 Whitehouse, M.J., 2008. Plešovice zircon — A new natural reference material for U-Pb
867 and Hf isotopic microanalysis. Chem. Geol. 249, 1–35.
868 doi:10.1016/j.chemgeo.2007.11.005

869 Smith, P.E., Tatsumoto, M., Farquhar, R.M., 1987. Zircon Lu-Hf systematics and the evolution of
870 the Archean crust in the southern Superior Province, Canada. Contrib. Mineral. Petrol. 97,
871 93–104.

872 Smithies, R.H., Van Kranendonk, M.J., Champion, D.C., 2005. It started with a plume – early
873 Archaean basaltic proto-continental crust. Earth Planet. Sci. Lett. 238, 284–297.

874 Söderlund, U., Patchett, P.J., Vervoort, J.D., Isachsen, C.E., 2004. The ^{176}Lu decay constant
875 determined by Lu-Hf and U-Pb isotope systematics of Precambrian mafic intrusions. Earth
876 Planet. Sci. Lett. 219, 311–324.

877 Stein, M., Hofmann, A.W., 1994. Mantle plumes and episodic crustal growth. Nature 372, 63–68.

878 Stevenson, R.K., Patchett, P.J., 1990. Implications for the evolution of continental crust from Hf
879 isotope systematics of Archean detrital zircons. Geochim. Cosmochim. Acta 54, 1683–
880 1697.

881 Stott, G.M., Davis, D.W., Parker, J.R., Straub, K.J., Tomlinson, K.Y., 2002. Geology and
882 tectonostratigraphic assemblages, eastern Wabigoon subprovince, Ontario. Geol. Surv.
883 Canada Open File 4285, 1 map sheet, scale 1:250,000.

884 Stott, G.M., Corkery, M.T., Percival, J.A., Simard, M., Goutier, J., 2010. A revised terrane
885 subdivision of the Superior Province. Ontario Geol. Surv. Open File Rep. 6260, 20-1 to
886 20-10.

887 Sundell, K., Saylor, J.E., Pecha, M., 2019. Provenance and recycling of detrital zircons from
888 Cenozoic Altiplano strata and the crustal evolution of western South America from
889 combined U-Pb and Lu-Hf isotopic analysis. In: Horton, B.K. and Folguera, A. (Eds)
890 Andean Tectonics (First Edition). Elsevier, 363–397.

891 Thirlwall, M.F., Anczkiewicz, R., 2004. Multidynamic isotope ratio analysis using MC-ICP-MS and
892 the causes of secular drift in Hf, Nd and Pb isotope ratios. Int. J. Mass Spectrom. 235, 59–
893 81.

894 Thurston, P.C., Ayer, J.A., Goutier, J., Hamilton, M.A., 2008. Depositional gaps in Abitibi
895 greenstone belt stratigraphy: A key to exploration for syngenetic mineralization. Econ.
896 Geol. 103, 1097–1134. doi:10.2113/gsecongeo.103.6.1097

897 Tomlinson, K.Y., Stott, G.M., Percival, J.A., Stone, D., 2004. Basement terrane correlations and
898 crustal recycling in the western Superior Province: Nd isotopic character of granitoid and
899 felsic volcanic rocks in the Wabigoon subprovince, N. Ontario, Canada. Precambrian Res.
900 132, 245–274. doi:10.1016/j.precamres.2003.12.017

901 Turek, A., Sage, R.P., Van Schmus, W.R., 1992. Advances in the U-Pb zircon geochronology of
902 the Michipicoten greenstone belt, Superior Province, Ontario. Can. J. Earth Sci. 29, 1154–
903 1165.

904 Van Kranendonk, M.J., Ivanic, T.J., Wingate, M.T.D., Kirkland, C.L., Wyche, S., 2013. Long-lived,
905 autochthonous development of the Archean Murchison Domain, and implications for
906 Yilgarn Craton tectonics. Precambrian Res. 229, 49–92.

907 Vervoort, J.D., Patchett, P.J., 1996. Behavior of hafnium and neodymium isotopes in the crust:
908 Constraints from Precambrian crustally derived granites. Geochim. Cosmochim. Acta 60,
909 3717–3733.

910 Vervoort, J.D., Blichert-Toft, J., 1999. Evolution of the depleted mantle: Hf isotopic evidence from
911 juvenile rocks through time. Geochim. Cosmochim. Acta 63, 533–556.

912 Vervoort, J.D., White, W.M., Thorpe, R.I., 1994. Nd and Pb isotope ratios of the Abitibi greenstone
913 belt: New evidence for very early differentiation of the Earth. Earth Planet. Sci. Lett. 128,
914 215–229.

915 Vervoort, J.D., Patchett, P.J., Söderlund, U., Baker, M., 2004. Isotopic composition of Yb and the
916 determination of Lu concentrations and Lu/Hf ratios by isotope dilution using MC-ICPMS.
917 Geochem. Geophys. Geosys. 5, Q11002. doi:10.1029/2004GC000721

918 Vezinet, A., Pearson, D.G., Thomassot, E., Stern, R.A., Sarkar, C., Luo, Y., Fisher, C.M., 2018.
919 Hydrothermally-altered mafic crust as source for early Earth TTG: Pb/Hf/O isotope and
920 trace element evidence in zircon from TTG of the Eoarchean Saglek Block, N. Labrador.
921 Earth Planet. Sci. Lett. 503, 95–107.

922 Vezinet, A., Pearson, D., Heaman, L.M., Sarkar, C., Stern, R.A., 2020. Early crustal evolution of
923 the Superior craton – A U-Pb, Hf and O isotope study of zircon from the Assean lake
924 complex and a comparison to early crust in other cratons. Lithos 368–369, 105600.
925 doi:10.1016/j.lithos.2020.105600

926 Walker, R.J., Shirey, S.B., Stecher, O., 1988. Comparative Re-Os, Sm-Nd and Rb-Sr isotope and
927 trace element systematics for Archean komatiite flows from Munro Township, Abitibi belt,
928 Ontario. Earth Planet. Sci. Lett. 87, 1–12.

929 Wiedenbeck, M., Allé, P., Corfu, F., Griffin, W.L., Meier, M., Oberli, F., von Quadt, A., Roddick,
930 J.C., Spiegel, W., 1995. Three natural zircon standards for U-Th-Pb, Lu-Hf, trace element
931 and REE analyses. Geostandards Newslett. 19, 1–23.

932 Zheng, Y.F., Wu, Y.B., Zhao, Z.F., Zhang, S.B., Xu, P., Wu, F.Y., 2005. Metamorphic effect on
933 zircon Lu-Hf and U-Pb isotope systems in ultrahigh-pressure eclogite-facies metagranite
934 and metabasite. Earth Planet. Sci. Lett. 240, 378–400.

935 Zirakparvar, N.A., Mathez, E.A., Rajesh, H.M., Choe, S., 2019. Lu-Hf isotopic evidence of a deep
936 mantle plume source for the ~2.06 Ga Bushveld Large Igneous Province. Lithos 348–349,
937 105168. doi:10.1016/j.lithos.2019.105168

Figure Captions

Fig. 1. Geology of the Superior Province displaying the distribution of predominantly magmatic subprovinces or domains colored by their oldest magmatic zircon ages and of primarily sedimentary subprovinces with depositional ages given in parentheses (modified from Stott et al., 2010).

Fig. 2. Schematic diagram illustrating the relative temporal and spatial relationships between gneissic-plutonic basement rocks, greenstone belt magmatism, granitic plutonism, deposition of successor basins, and phases of shortening deformation from north to south in the Superior Province. Temporal relationships are simplified using a wide variety of methods (field relationships, U-Pb dating of zircon, Hf and Nd model ages, etc.) and published studies (after Percival et al., 2012, and references therein).

Fig. 3. Map of the Abitibi and Pontiac subprovinces displaying the distribution of volcanic assemblages, mafic and felsic to intermediate intrusions, and primary sedimentary assemblages. The locations of detrital zircon samples investigated in the present study are given. Modified from Thurston et al. (2008) and Monecke et al. (2017).

Fig. 4. Cathodoluminescence images of representative detrital zircon grains analyzed from successor basin rocks of the Abitibi and Pontiac subprovinces organized by age from youngest to oldest. The analysis locations, sample/spot reference numbers, $^{207}Pb/^{206}Pb$ ages, and ε_{Hf} values for each grain are labeled. Indicated uncertainty for all analyses is 2σ.

Fig. 5. Frequency histograms (rectangles), probability density function curves (filled solid colored lines), and cumulative distribution function curves (solid and dashed lines) for U-Pb zircon data in the study region. (A) Selected concordant $^{207}Pb/^{206}Pb$ ages of detrital zircon grains from the Abitibi and Pontiac subprovinces from Frieman et al. (2017) on which Lu-Hf analyses were performed (this study). (B) Compilation of published U-Pb zircon age data for volcanic-plutonic rocks of the

Abitibi subprovince and adjacent domains in the southern Superior Province (Winnipeg River, Marmion, and Opatica subprovinces) (modified from Frieman et al., 2017). The published age data for volcanic-plutonic rocks of the Abitibi subprovince (solid green line) do not perfectly match the detrital zircon age pattern observed in successor basin samples of the Abitibi and Pontiac subprovinces (black dashed line). However, the observed distribution of ages in our samples can be explained by a component of mixing between Abitibi and older source rocks (southern Superior; purple irregular dashed line).

Fig. 6. Plots displaying the isotopic results obtained by LA-MC-ICP-MS analysis of detrital zircon grains from Abitibi and Pontiac subprovince successor basin samples in this study. (A) The ε_{Hf} - $^{207}Pb/^{206}Pb$ age results. Error bars in are 2σ uncertainty. (B) A bivariate histogram plot of the data displayed in (A) using 10 Ma and 0.5 ε_{Hf} unit bin spacing. An approximate average 2σ uncertainty is indicated, and groups with similar distributions are outlined (see text for detailed descriptions of the group subdivisions labelled 1-6). The vertical gray bar represents the approximate age threshold between Abitibi (younger) and non-Abitibi (older) ages. The green line represents the evolution of depleted mantle (DM) compositions as calculated from modern MORB values of Griffin et al. (2002). The purple line corresponds to compositions of the chondritic uniform reservoir (CHUR). Gray dashed lines represent ε_{Hf} growth curves calculated using $^{176}Lu/^{177}Hf$ = 0.015, which is the approximate mid-point between reported end-member values for crustal mafic rocks (0.022; Amelin et al., 1999) and Precambrian granitoid rocks (0.0093; Vervoort and Patchett, 1996). This value also coincides with the average crustal composition of the Superior Province as derived from whole-rock geochemical analyses of sedimentary rocks (Stevenson and Patchett, 1990).

Fig. 7. Plots displaying previously published paired Hf (A-B) and Nd (C-D) isotopic and age data for the southern Superior Province. (A) $^{207}Pb/^{206}Pb$ age and ε_{Hf} zircon data from the Abitibi (Corfu and Noble, 1992; Ketchum et al., 2008) and Wawa (Smith et al., 1987; Bjorkman, 2017)

subprovinces. (B) $^{207}Pb/^{206}Pb$ age and ε_{Hf} zircon data from the Quetico, Western Wabigoon, Marmion, and Winnipeg River (Davis et al., 2005; Bjorkman, 2017) subprovinces. (C) $^{207}Pb/^{206}Pb$ age and whole-rock ε_{Nd} data for the Abitibi (Cattell et al., 1984; Dupré et al., 1984; Shirey and Hanson, 1986; Walker et al., 1988; Vervoort et al., 1994; Vervoort and Blichert-Toft, 1999) and Wawa (Polat and Kerrich, 2002; Polat, 2009; Lodge, 2016) subprovinces. (D) $^{207}Pb/^{206}Pb$ age and whole-rock ε_{Nd} data for the Western Wabigoon (Beakhouse and McNutt, 1991; Larbi et al., 1999; Ayer and Dostal, 2000), Marmion (Tomlinson et al., 2004), and Winnipeg River (Henry et al., 2000; Tomlinson et al., 2004) subprovinces. Vertical gray bars represent the approximate age threshold between Abitibi (younger) and non-Abitibi (older) ages. See Fig. 6 for a description of the parameters used to calculate the depleted mantle (DM) and ε_{Hf} growth curves shown in (A) and (B). The previously published Hf isotope compositions displayed in (A) and (B) were calculated using the same reference parameters as those used is this study (see section 3). Initial ε_{Nd} values displayed in (C) and (D) were calculated based on chondritic uniform reservoir (CHUR) values of $^{147}Sm/^{144}Nd$ = 0.1960 and $^{143}Nd/^{144}Nd$ = 0.512630 (Bouvier et al., 2008). The DM evolution curves displayed in (C) and (D) were calculated from modern day MORB-DM values of $^{147}Sm/^{144}Nd$ = 0.2135 and $^{143}Nd/^{144}Nd$ = 0.513151 (ε_{Nd} = +10) after DePaolo and Wasserburg (1976) and Pearson et al. (1995).

Fig. 8. Plot comparing the statistical distribution of $^{207}Pb/^{206}Pb$ age and ε_{Hf} data from the southern Superior Province. All Gaussian, bivariate population density distributions were calculated in HafniumPlotter v1.7 (Sundell et al., 2019) using a kernel density spacing of 0.5 ε_{Hf} and 10 Ma. Colored fields reflect detrital zircon data from this study: 100% of data (blue), data falling within ~95% of the mean (yellow), and all data falling within ~68% of the mean (red). The dashed lines represent published data for the Abitibi and Wawa subprovinces (purple; Smith et al., 1987; Corfu and Noble, 1992; Ketchum et al., 2008; Bjorkman, 2017) and southwestern Superior Province (blue; western Wabigoon, Winnipeg River, and Marmion subprovinces; Davis et al., 2005;

1012 Bjorkman, 2017); thin dashed lines represent all data within ~95% of the population mean, and
1013 thick dashed lines all data within ~68% of the population mean. The previously published results
1014 and data from this study were both calculated using the same reference parameters (see section
1015 3). The secular age-Hf isotope patterns are inferred to reflect crustal growth in the southern
1016 Superior Province from a primarily chondritic source at >3000 Ma (blue bar) and an isotopically
1017 distinct, depleted mantle source at ~3000–2700 Ma (green bar). More evolved, statistically
1018 subordinate CHUR-like to negative values are interpreted to reflect internal reworking of older
1019 crust and/or mixing of evolved crust with juvenile, depleted mantle inputs during progressive
1020 growth and regional amalgamation events. Statistically minor, strongly-depleted signatures are
1021 interpreted to reflect volumetrically minor crust or mantle source domains that experienced multi-
1022 stage melt depletion histories.

1023 **Fig. 9.** Measured $^{232}Th/^{238}U$ ratios versus $^{232}Th/^{238}U$ ratios calculated from measured $^{208}Pb/^{206}Pb$
1024 ratios for a representative subset of analyses from groups 1 and 2 (A), groups 3 and 4 (B), and
1025 groups 5 and 6 (C). The 2σ uncertainty is less than symbol size.

1026 **Table 1.** List of graywacke samples from successor basins of the Abitibi and Pontiac subprovinces
1027 used for U-Pb and Lu-Hf LA-ICP-MS detrital zircon analysis.

Figure 1

Click here to access/download;Figure;Fig. 1.tif

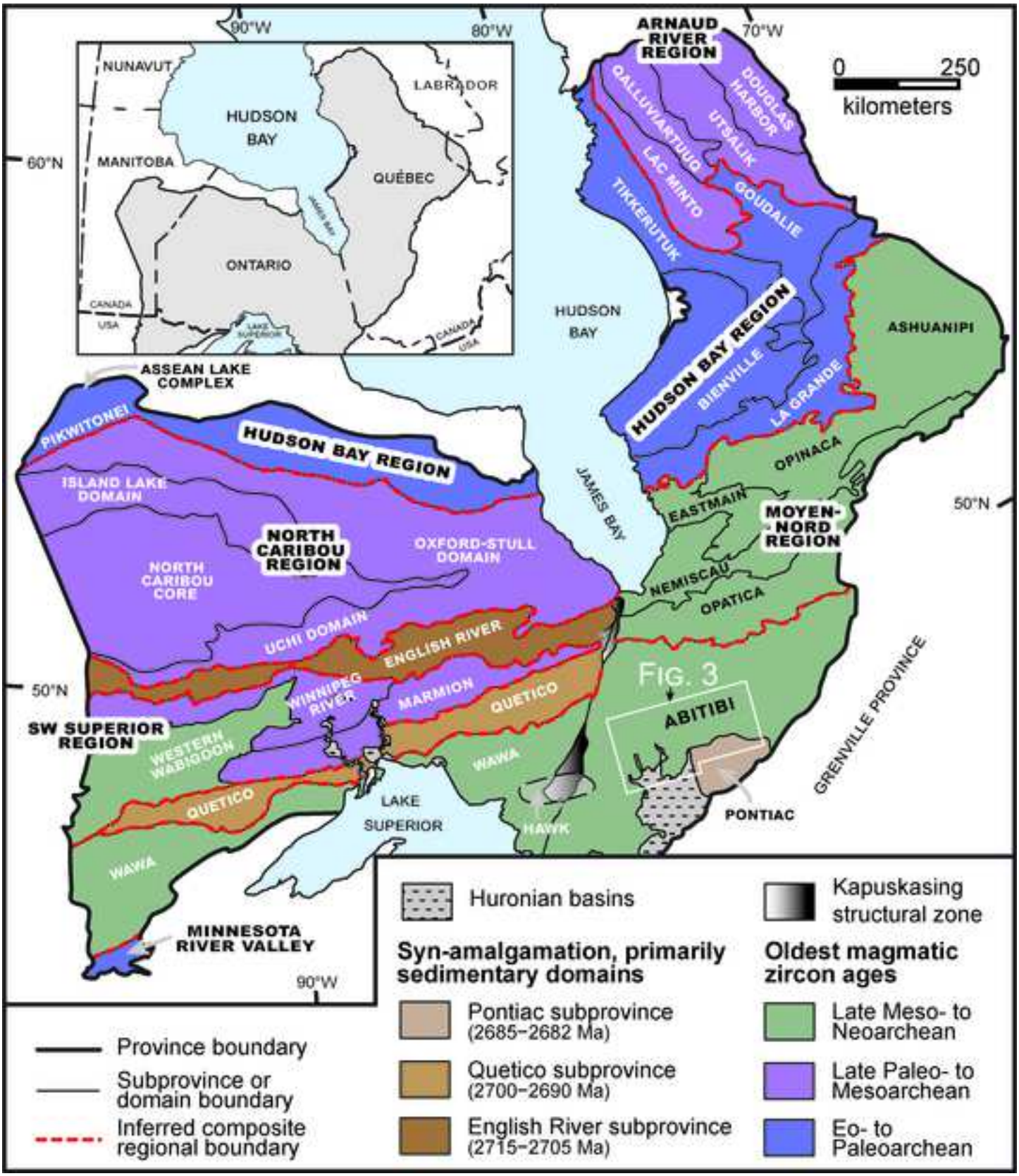

Figure 2

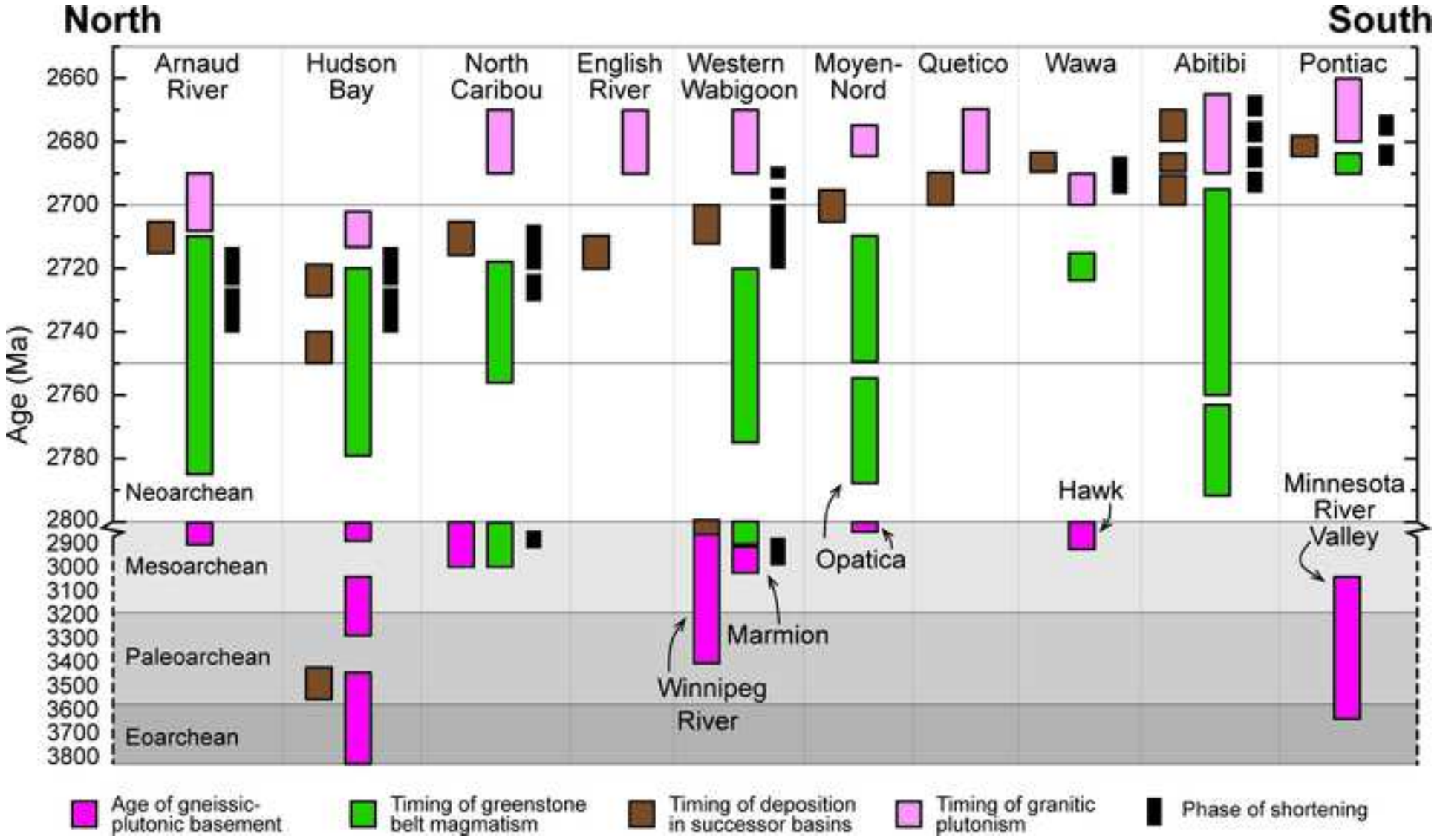

Figure 3

Click here to access/download;Figure;Fig. 3.tif

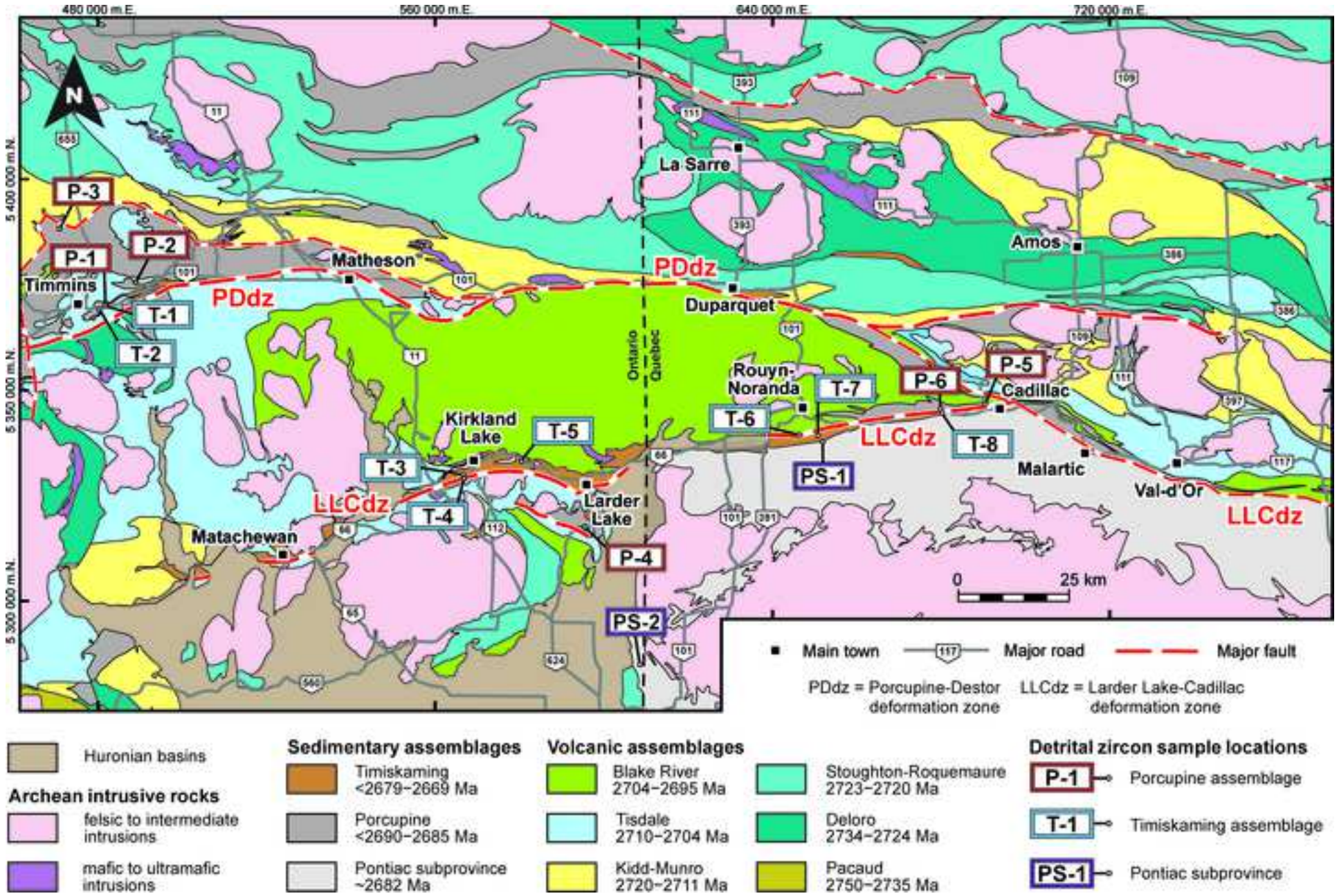

Figure 4

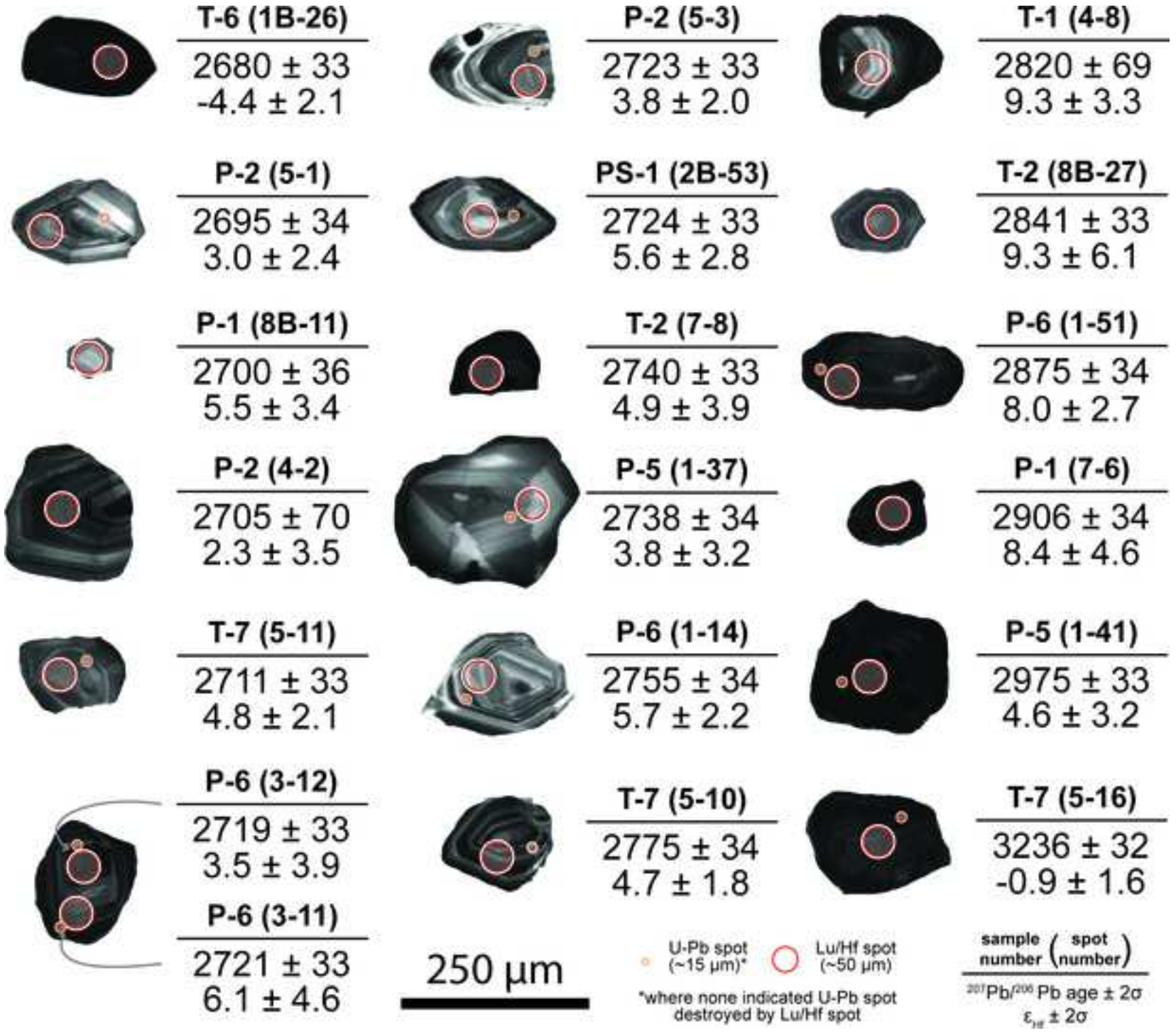

Figure 5

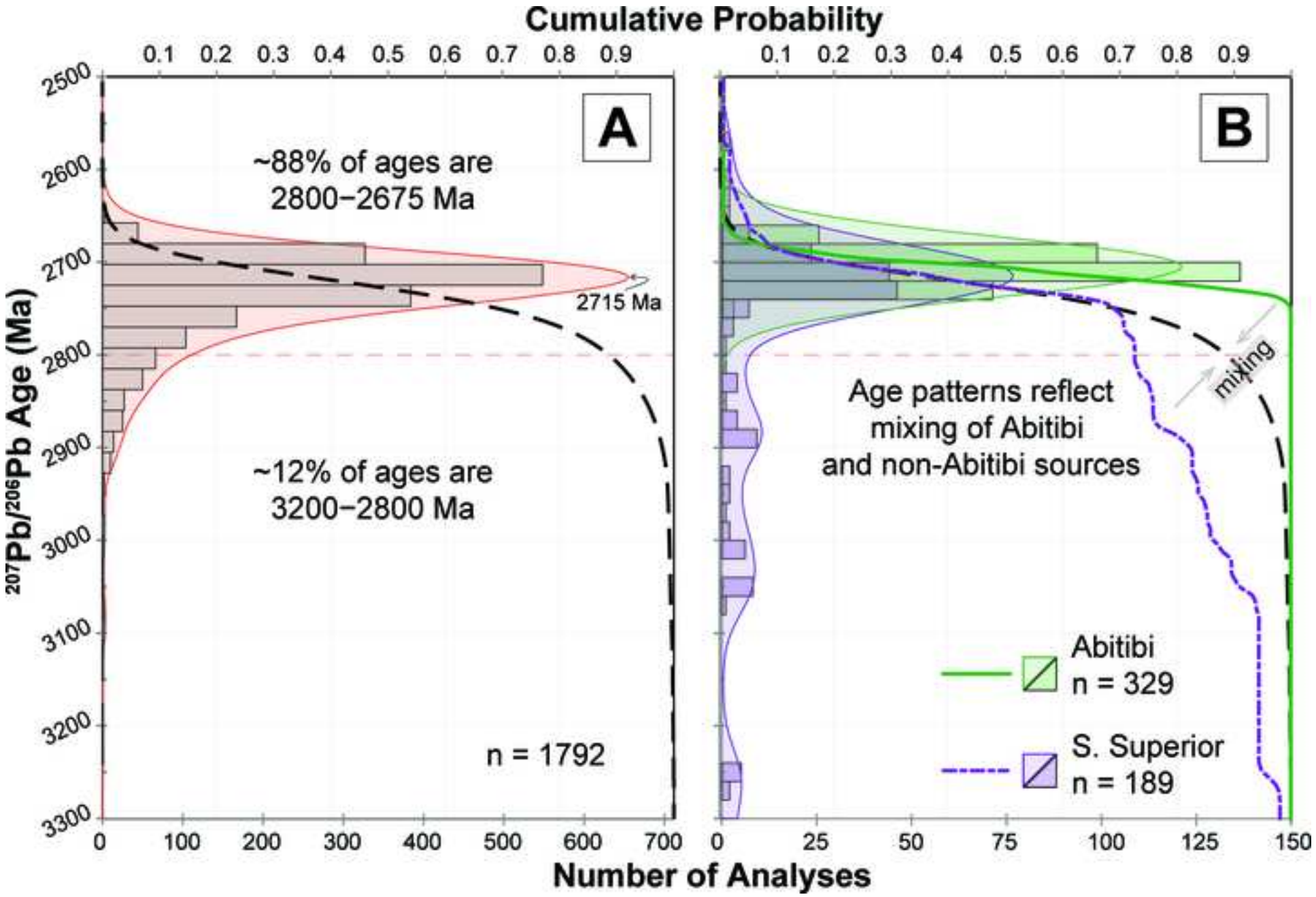

Figure 6

Click here to access/download;Figure;Fig. 6.tif

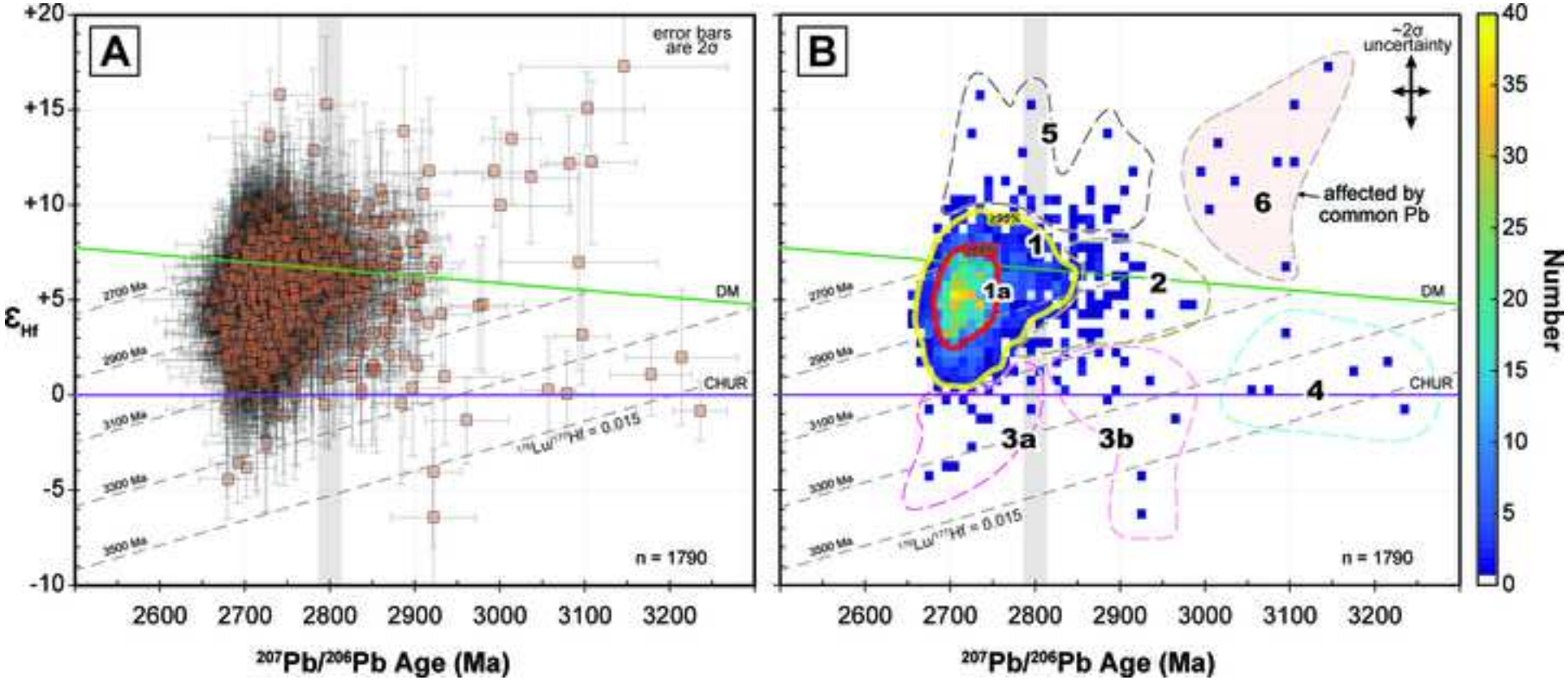

Figure 7

Click here to access/download;Figure;Fig. 7.tif

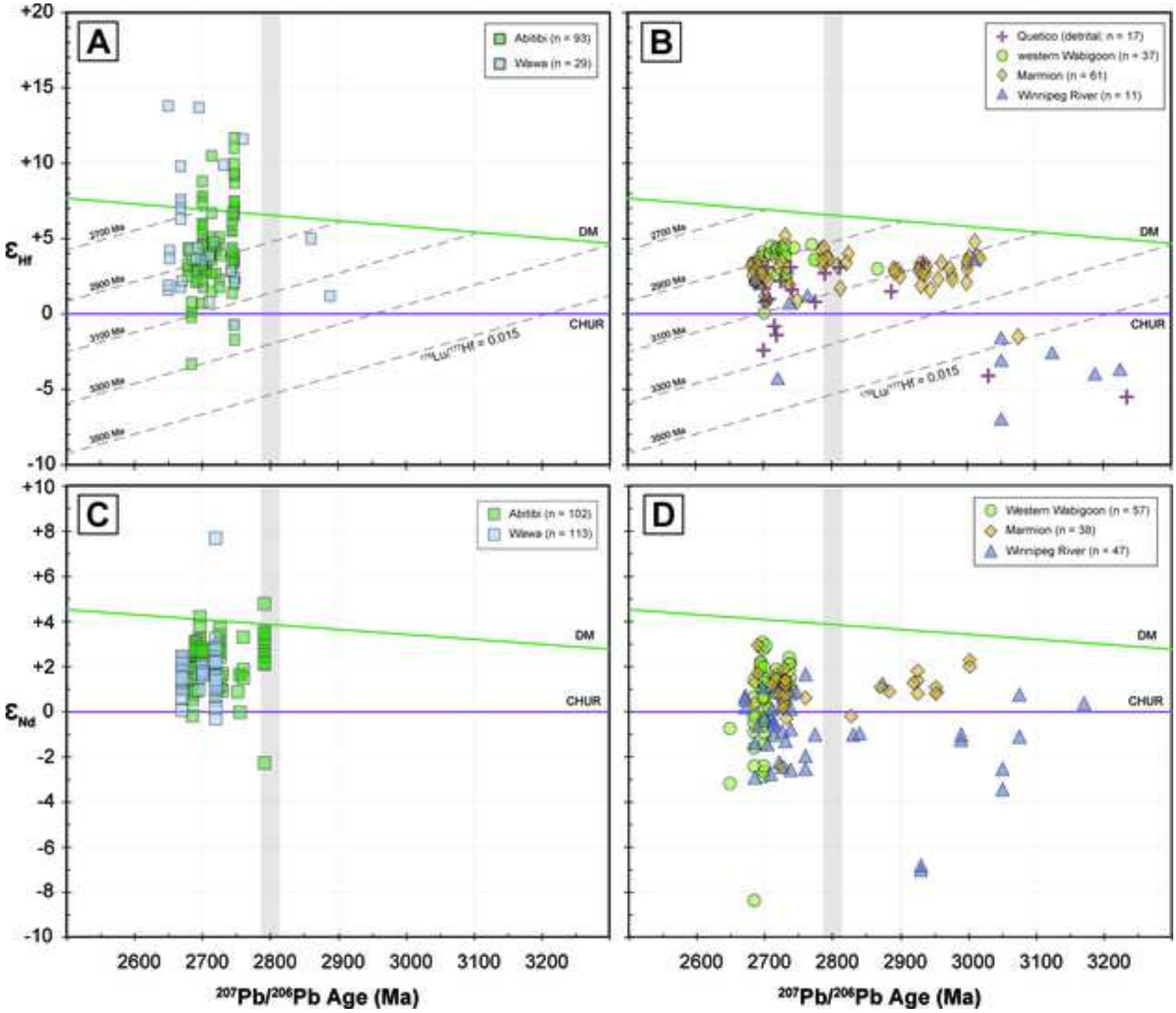

Figure 8

Click here to access/download;Figure;Fig. 8.tif

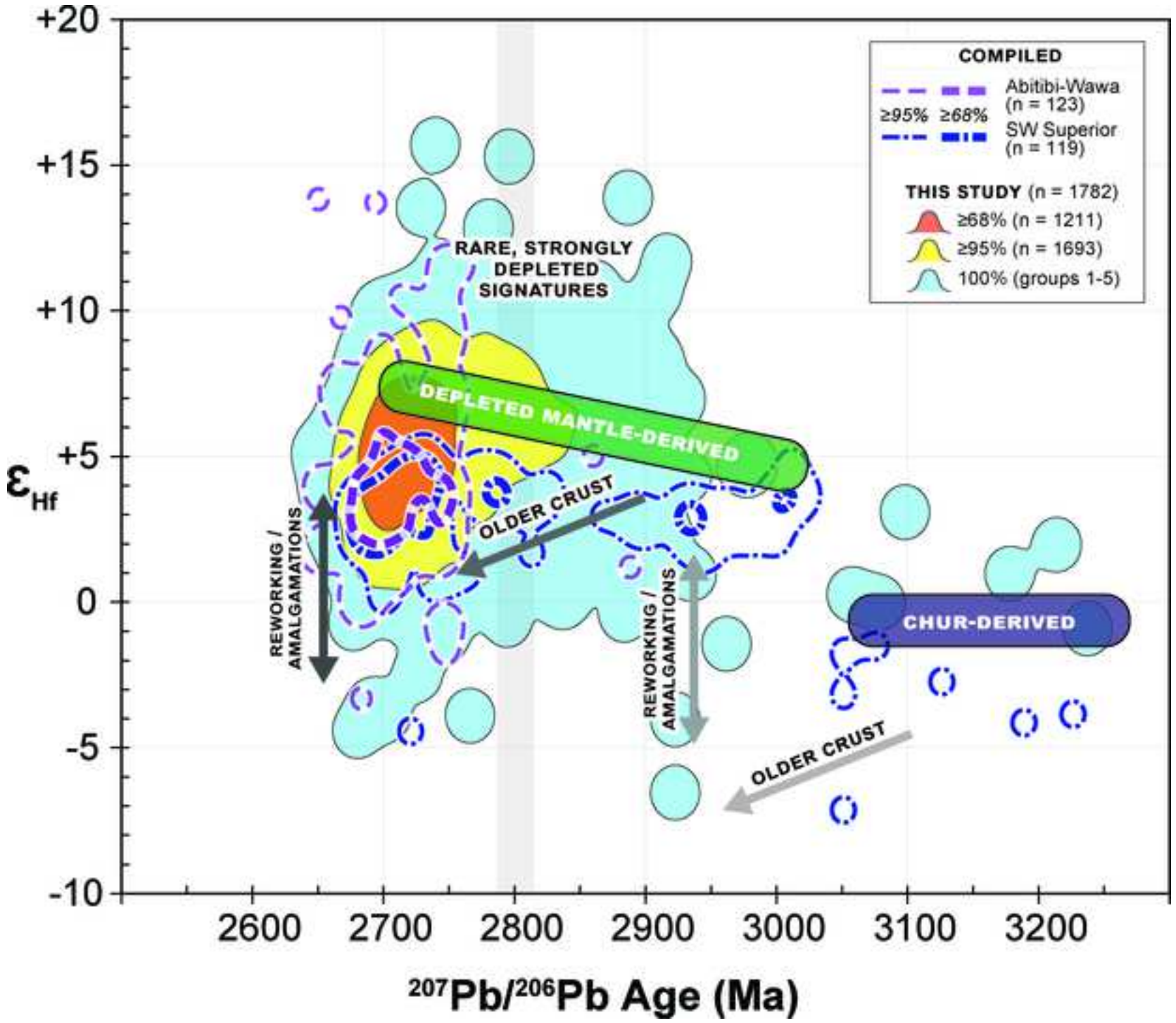

Figure 9

Click here to access/download;Figure;Fig. 9.tif

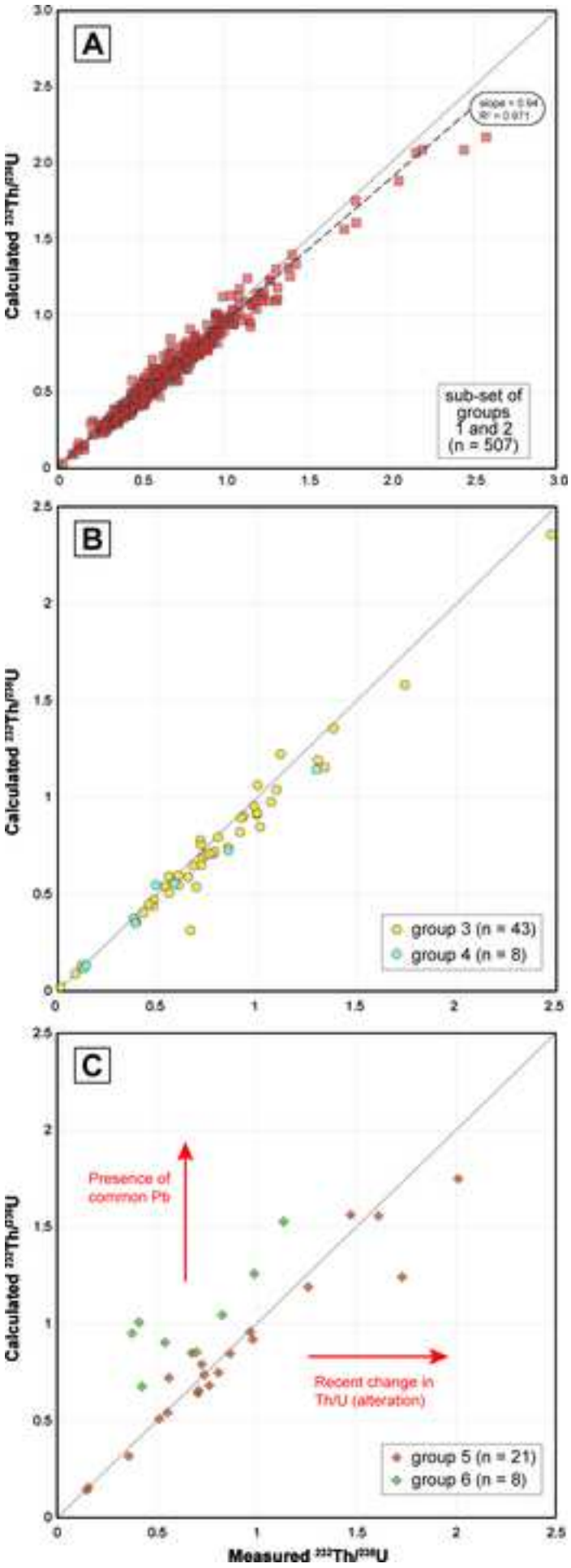

Table 1

	Sample #	Location	UTM zone (NAD83)	Northing (m)	Easting (m)
Porcupine assemblage	P-1	Timmins	17U	5371274	484261
	P-2	Timmins	17U	5377126	493189
	P-3	Timmins	17U	5393390	473340
	P-4	Larder Lake	17U	5318272	597448
	P-5	LaRonde Penna	17U	5346548	690224
	P-6	LaRonde Penna	17U	5345265	680339
Pontiac subprovince	PS-1	Rouyn-Noranda	17U	5337608	651829
	PS-2	western Pontiac subprovince	17T	5285124	610613
Timiskaming assemblage	T-1	Timmins	17U	5371207	484998
	T-2	Timmins	17U	5369513	483540
	T-3	Kirkland Lake	17U	5331699	569426
	T-4	Kirkland Lake	17U	5330831	570190
	T-5	Morris-Kirkland	17U	5333712	580331
	T-6	Rouyn-Noranda	17U	5339898	646428
	T-7	Rouyn-Noranda	17U	5340052	650339
	T-8	LaRonde Penna	17U	5344928	680437

Conflict of Interest Statement

The authors declare that there is no conflict of interest.

Author CRediT statement

Ben M. Frieman: Conceptualization, investigation, Writing – original draft, visualization, data curation, formal analysis

Nigel Kelly: Conceptualization, investigation, Writing – Original Draft, supervision, funding acquisition

Yvette D. Kuiper: Conceptualization, Writing – review & editing, supervision, funding acquisition

Thomas Monecke: Writing – review & editing, funding acquisition

Andrew Kylander-Clark: Methodology, resources, validation

Martin Guitreau: Writing – review & editing